The behaviour of highly siderophile elements in oceanic crust during subduction: whole-rock and mineral-scale insights from a high-pressure terrain

C.W. Dale[a,b*], K.W. Burton[b∞], D.G. Pearson[a], A. Gannoun[b∞], O. Alard[b#], T.W. Argles[b], I.J. Parkinson[b]

[a]*Department of Earth Sciences, Durham University, Science Laboratories, Durham, DH1 3LE, UK*

[b]*Department of Earth Sciences, CEPSAR, The Open University, Walton Hall, Milton Keynes, MK7 6AA, UK*

[∞] *current address: Dept of Earth Sciences, Oxford University, Oxford, OX1 3PR, UK*

 # current address: Univ Montpellier 2, CNRS, UMR 5243, CC 60, F-34095 Montpellier, France

[*]corresponding author. email: christopher.dale@durham.ac.uk. Tel: +44 0191 3342338, Fax: +44 0191 3342301

ABSTRACT

Highly siderophile element concentrations (HSE: Re and platinum-group elements (PGE)) are presented for gabbros and gabbroic eclogites and basaltic eclogites from the high-pressure Zermatt-Saas ophiolite terrain, Switzerland. Rhenium and PGE (Os, Ir, Ru, Pt, Pd) abundances in gabbro- and eclogite-hosted sulphides, and Re-Os isotopes and elemental concentrations in silicate phases are also reported. This work, therefore, provides whole-rock and mineral-scale insights into the PGE budget of gabbroic oceanic crust and the effects of subduction metamorphism on gabbroic and basaltic crust.

Chondrite-normalised PGE patterns for the gabbros are similar to published mid-ocean ridge basalts (MORB), but show less inter-element fractionation. Mean Pt and Pd contents of 360 and 530 pg/g, respectively, are broadly comparable to MORB, but gabbros have somewhat higher abundances of Os, Ir and Ru (mean: 64, 57 and 108 pg/g). Transformation to eclogite has not significantly changed the concentrations of the PGE, except Pd which is severely depleted in gabbroic eclogites relative to gabbros (~75% loss). In contrast, basaltic eclogites display significant depletion of Pt (≥60%), Pd (>85%) and Re (50-60%) compared with published MORB, while Os, Ir and Ru abundances are broadly comparable. Thus, these data suggest that only Pt, Pd and Re, and not Os, Ir and Ru, may be significantly fluxed into the mantle wedge from mafic oceanic crust. Re-Os model ages for gabbroic and gabbroic eclogite minerals are close to age estimates for igneous crystallisation and high-pressure metamorphism, respectively, hence the HSE budgets can be related to both igneous and metamorphic behaviour. The gabbroic budget of Os, Ir, Ru and Pd (but not Pt) is dominated by sulphide, which typically hosts >90% of the Os, whereas silicates account for most of the Re (with up to 75% in plagioclase alone). Sulphides in gabbroic eclogites tend to host a smaller proportion of the total Os (10-90%) while silicates are important hosts, probably

reflecting Os inheritance from precursor phases. Garnet contains very high Re concentrations and may account for >50% of Re in some samples. The depletion of Pd in gabbroic eclogites appears linked, at least in part, to the loss of Ni-rich sulphide.

Both basaltic and gabbroic oceanic crust have elevated Pt/Os ratios, but Pt/Re ratios are not sufficiently high to generate the coupled ^{186}Os-^{187}Os enrichments observed in some mantle melts, even without Pt loss from basaltic crust. However, the apparent mobility of Pt and Re in slab fluids provides an alternative mechanism for the generation of Pt- and Re-rich mantle material, recently proposed as a potential source of ^{187}Os-^{186}Os enrichment.

Keywords: platinum-group elements (PGE), rhenium, osmium, gabbro, MORB, oceanic crust, subduction, recycling, metasomatism, element mobility, sulphide and silicate minerals.

1. INTRODUCTION

The platinum group elements (PGE: Os, Ir, Ru, Rh, Pt, and Pd) and Re are highly siderophile elements (HSE) that provide key information on the differentiation of the early Earth and the subsequent evolution of the silicate mantle. During core-mantle separation, the 'metal-loving' siderophile elements are strongly partitioned into the metallic core, leaving a highly depleted silicate mantle. However, actual mantle siderophile element abundances are much higher than might be expected for low pressure-temperature (P-T) metal-silicate equilibration (Borisov et al., 1994; Righter and Drake, 1997; Ertel et al., 1999; Holzheid et al., 2000), most likely due to high P-T silicate-metal equilibration or heterogeneous accretion (the so-called late veneer, Chou, 1978), where continued accretion of meteoritic material, after core formation, replenished the HSE.

The HSE are also chalcophile ('sulphur-loving') and hence strongly partitioned into sulphide minerals in the silicate mantle itself. Sulphide is generally thought to be a residual phase during moderate mantle melting (e.g. <20%, during the generation of Mid-Ocean Ridge Basalts (MORB)), and those melts are also commonly sulphur saturated prior to or during eruption, resulting in sulphide crystallisation during magmatic differentiation (e.g. Lorand et al., 1999; Luguet et al., 2003; Bezos et al., 2005). Thus, the HSE are preferentially retained in residual sulphide in the mantle during melting, and further removed from such melts during the crystallisation and segregation of magmatic sulphide. Available data indicate that during magmatic crystallisation sulphide/melt partition coefficients are of a similar order of magnitude for all of the PGE (e.g. Peach et al., 1990; Fleet et al., 1996). In contrast, experimental and natural observations of mantle sulphides suggests that they melt incongruently releasing a Cu-Ni rich sulphide melt, and leaving a refractory Fe-Ni monosulphide solid solution that concentrates Os, Ir and Ru, relative to Pt, Pd and Re (e.g.

Alard et al., 2000; Bockrath et al., 2004; Peregoedova et al., 2004). Thus, the HSE variations in MORB are consistent with the widely accepted order of decreasing compatibility, from highly compatible for Os and Ir, through Ru, Pt, and Pd, to moderately incompatible for Re (e.g. Barnes et al., 1985).

Amongst the HSE, Re and Os are linked through β-decay of ^{187}Re to ^{187}Os. Due to the marked difference in compatibility during mantle melting, both oceanic and continental crust possess very high Re/Os ratios relative to the silicate mantle, and over time evolve to radiogenic Os isotope compositions. Consequently, the Re-Os isotope system potentially serves as an exceptional tracer of recycled crustal material in the convective mantle. However, recent studies have shown that during high-pressure (eclogite-facies) metamorphism accompanying subduction, Re and Os exhibit differential mobility between different rock types in the oceanic crust. Basalts show evidence for significant Re mobility and loss (50-60%, Becker, 2000; Dale et al., 2007) whereas gabbros preserve Re-Os isotope signatures consistent with little mobility of either element subsequent to igneous crystallisation (Dale et al., 2007). Such differential behaviour most likely relates to the degree of hydration of the original rock type and its deformation history, but variable behaviour of the mineral assemblage, particularly sulphides (the principal host for many HSE), may also play a role. However, the distribution and behaviour of other platinum-group elements (PGE) in the oceanic crust (both gabbro and basalt) remain poorly constrained (cf. Lorand and Juteau, 2000), as does their behaviour during high-pressure metamorphism accompanying subduction, and it is not clear to what extent HSE abundances in the silicate mantle may be affected by the recycling of oceanic crust, and in particular the extent to which Pt and Re mobility could potentially generate coupled ^{186}Os-^{187}Os enrichments observed in some mantle melts.

This study presents HSE abundances and Re-Os isotope data for basalts and gabbros from the Zermatt-Saas ophiolite, metamorphosed to eclogite-facies conditions during the Alpine orogeny. This includes whole rock and mineral data (silicate, oxide and sulphide) for gabbroic eclogites and their un-metamorphosed igneous precursors, and whole rock data for basaltic eclogites. As no precursor basalt has been preserved, basaltic eclogite data have been compared to MORB. These results provide the first insight into the distribution of HSE in gabbroic and basaltic crust (and amongst gabbroic minerals) and their behaviour during high pressure metamorphism, with the potential consequences for their redistribution in the subduction zone environment and recycling into the mantle.

2. GEOLOGICAL SETTING, SAMPLE PETROGRAPHY and P-T ESTIMATES (smaller type possible)

Samples were collected from the Zermatt-Saas ophiolite (ZSO), Switzerland, which originally formed part of the Mesozoic Tethyan oceanic crust (~164 Ma, Rubatto et al., 1998). The ZSO underwent Eocene high- to ultra-high pressure (UHP) metamorphism during south-easterly directed subduction and the subsequent continental collision that formed the Alpine mountain belt. Sampling of the variably metamorphosed Allalin Gabbro body and nearby metabasaltic eclogite units (Täschalp-Pfulwe) was aimed at retrieving lithologies representative of the mafic lower and upper oceanic crust, much of which was recrystallised under metamorphic conditions comparable to those present in subduction zones. Details of sampling area and localities can be found in Dale et al. (2007).

2.1 Petrology and silicate mineralogy

Samples of gabbroic origin preserve a range of *apparent* metamorphic conditions, although field (and even hand-specimen) evidence indicates that all parts of the Allalin unit experienced similar eclogite-facies P-T conditions. In some cases, the magmatic mineralogy of the gabbros, principally forsterite-rich olivine, augite and labradoritic plagioclase (compositions in Table EA-1, electronic annex), is preserved entirely. This metastable preservation probably results from the local absence of fluid infiltration, anhydrous mineralogy and a relatively low peak temperature (~600°C, see below). In contrast, other samples from the same body have recrystallised entirely during metamorphism and comprise an eclogite-facies mineralogy (including garnet, omphacite, zoisite, paragonite, talc and glaucophane, Table EA-1). Although a complex spectrum exists, most gabbros and gabbroic eclogites chosen for this study represent the two endmembers. However, several samples from the Allalin Gabbro display a transition from gabbro to metagabbro/eclogite on the scale of an individual hand specimen (referred to as transitional gabbros). These samples probably experienced some fluid infiltration and recrystallisation during seafloor metamorphism (see below) and further recrystallisation during HP metamorphism, but both transformations are incomplete. The utility of such samples, and this gabbroic body as a whole, is the opportunity to directly compare the chemistry of unmodified gabbros with genetically-related eclogite equivalents, without the uncertainties that typically arise when comparing igneous materials with differing sources and magmatic history.

Little or no greenschist-facies retrogression is evident in the gabbroic eclogites chosen. Samples were not taken from the more deformed edges of the Allalin body, which display greater retrogression, and consequently the sample suite may have a bias towards less deformed samples which may have experienced less fluid flow during prograde

metamorphism. However, all eclogites experienced fluid infiltration, probably initially during seafloor alteration (oxygen isotope evidence, Barnicoat and Cartwright, 1997). Basaltic eclogites consist entirely of metamorphic minerals: garnet, omphacite, zoisite, glaucophane, phengite +/- paragonite, and retrograde barroisitic amphibole. Some of the metabasalts display variable greenschist retrogression (<20%), but it is considered unlikely that the samples have been extensively chemically modified during exhumation.

2.2 Sulphide and oxide mineralogy

Accessory oxides and sulphides combined constitute less than 2% of each whole rock. Ilmenite and Al-chromite (variable Cr number: 0.46 and 0.74 in two different samples) are present in most of the gabbros studied, while both are absent from the gabbroic eclogites. An Fe-rich sulphide (pyrrhotite, Po), Ni-rich sulphide (pentlandite, Pn) and Cu-rich sulphide (chalcopyrite, Cp) are all present in the gabbros, with pyrrhotite constituting 60-90% of total sulphide in the three samples for which PGE in sulphide have been determined (e.g. Figure 1). Some (original?) pyrrhotite has been altered to troilite which, combined with Fe-rich pentlandite and chalcopyrite, may suggest a degree of alteration under mildly reducing conditions (Lorand, 1985). Pentlandite and chalcopyrite occur in modal proportions of ~10-30% and <10%, respectively. An important distinction in sulphide mineralogy is the predominance of pyrite in the gabbroic eclogites (50-100%), and its absence in the gabbros. Pyrrhotite and chalcopyrite are also present in the gabbroic eclogites, but are much less common (1-45% and <5%, respectively), while pentlandite is absent. Typical major element compositions of the sulphide phases are given in Table 1.

Figure 1 here.

Table 1 here.

Gabbroic sulphides range in diameter from 1 to 500 μm and occur both as small inclusions within silicate phases or in larger forms at grain boundaries between all the major silicates. All sulphides occur as massive grains and no exsolution flames have been observed. Olivine crystals contain numerous tiny opaque inclusions (<2 μm) which lie along internal fracture surfaces within the crystals, these comprise the three igneous sulphide phases (Po, Pn, Cp) and at least one oxide phase (probably chromite given its early crystallisation), but their size precludes LA-ICP-MS analysis. Gabbroic eclogite sulphides are less numerous but typically much larger than those in gabbros (800 x 1000 μm in one case, Figure 1), suggesting recrystallisation in a hydrothermal or metamorphic fluid. The occurrence of transitional monoclinic/hexagonal pyrrhotite, together with pyrite and chalcopyrite, is inconsistent with low temperature (<250°C) equilibration (Kissin and Scott, 1982) and thus suggests formation during high-temperature hydrothermal alteration or HP metamorphism, with partial inversion to a monoclinic habit during cooling. Such an assemblage indicates relatively oxidising conditions, possibly in the presence of Fe-poor pyroxene (Harlov et al., 1997), a constituent of an eclogitic assemblage. The absence of either euhedral single-phase pyrite grains or sulphur gain in the gabbroic eclogites also strongly suggests a metamorphic origin for the eclogite sulphide assemblage (Luguet et al., 2004).

Metamorphic recrystallisation of basaltic sulphides has also resulted in the formation of pyrite at the expense of igneous sulphide phases. Pyrrhotite and pentlandite have not been identified in metabasalts but minor chalcopyrite remains (<10%). As there is no basaltic protolith preserved, the identity of initial sulphide phases is uncertain, but observations of other MORB (e.g. Czamanske and Moore, 1977; Roy-Barman et al., 1998) and the gabbros in this study suggest that an Fe-rich (monosulphide solid solution (mss) or pyrrhotite), Ni-rich (pentlandite) and Cu-rich sulphide (chalcopyrite or intermediate solid solution (iss)) would have been present. Chalcopyrite may have been present in greater proportion in the precursor

basalts than in the cumulate gabbros, given that MORB sulphide globules display positively co-varying Ni/Cu and Mg number (Czamanske and Moore, 1977), presumably due to the lower and higher solidi of Cu-rich and Fe-Ni-rich sulphide liquids, respectively. Unlike the gabbroic samples, sulphides in basaltic eclogites display minor alteration to haematite (<15%).

2.3 Pressure-Temperature-time estimates for high-pressure metamorphism

Pressure (P) – temperature (T) estimates for the equilibration of mineral assemblages in gabbroic and basaltic eclogites have been obtained using the internally-consistent thermodynamic dataset (THERMOCALC® program) of Holland & Powell (1985; 1990; 1998) and Powell & Holland (1985; 1988). As igneous compositional domains are retained in some gabbroic eclogites, indicating disequilibrium, P-T estimates in these cases were generated from individual domain assemblages and surrounding garnet coronas.

The peak metamorphic assemblage for gabbroic eclogites is typically garnet + omphacite + paragonite + actinolite + clinozoisite + quartz ± chloritoid + fluid (CO_2-H_2O, x(H_2O) = 0.8). Pressure estimates range from 1.9 to 2.2 GPa, while temperature varies between 500 and 580°C, similar to previous estimates for the Allalin Gabbro and Täschalp (Pfulwe) areas in the northern ZSO (≥2.0 GPa and 550-600°C, Meyer, 1983; Barnicoat and Fry, 1986), but lower than those for the Lago di Cignana area to the south (2.7-2.9 GPa and 600-630°C, Reinecke, 1991). However, on the basis of carbonate phase equilibria, it has been suggested that peak metamorphic pressures for the Allalin Gabbro may have reached 3.5 GPa (Barnicoat, 1996). The assemblage in basaltic eclogites typically comprises garnet + omphacite + muscovite + paragonite + glaucophane + clinozoisite + quartz + fluid (CO_2-H_2O, x(H_2O) = 0.8). The P-T estimates for this assemblage are comparable to those for gabbroic eclogites and vary between 1.9-2.2 GPa and 530-600°C, respectively. The significance of

such P-T conditions is that they are comparable to those typical of present-day subduction zones, where temperatures remain low for a given pressure.

Garnet Sm-Nd and metamorphic zircon U-Pb data yield ages for peak metamorphism of 40.6±2.6 Ma (Amato et al., 1999) and 44.1±0.7 Ma (Rubatto et al., 1998), respectively. A retrogressive greenschist facies age of 38±2 Ma (Rb-Sr) has been estimated, suggesting initially rapid exhumation (10-26 km/Ma, Amato et al., 1999) which evidently aided preservation of the high pressure assemblage with very little retrograde metamorphism.

2.4 Summary of published major and trace element chemistry

The major and trace element chemistry of the samples in this study has been previously described by Dale et al. (2007). Although the samples have been chemically altered by pervasive HP-LT metamorphism, the less 'fluid-mobile' elements such as the mid to heavy REE suggest an E-MORB-like initial composition for the basaltic eclogites (Dale et al., 2007). The chemistry of the gabbroic lithologies reflects their formation by crystal accumulation, particularly plagioclase (e.g. positive Sr, Ba and Eu anomalies). Whole-rock large-ion lithophile element (LILE: Ba, Rb, K) abundances have been depleted by up to 80% in both gabbroic and basaltic eclogites when compared to so-called 'fluid-immobile' elements such as Nb (Dale et al., 2007). Strontium is also depleted, particularly in the gabbroic eclogites, while there is apparently no loss of U from either gabbroic or basaltic material, possibly due to zircon growth during metamorphism.

3. ANALYTICAL TECHNIQUES (smaller type possible)

Whole-rocks. Whole rock powders (~1-2g;) were ground in agate, following crushing within plastic by hammer (to avoid steel contamination), and were digested and equilibrated with a mixed ^{190}Os–^{191}Ir–^{99}Ru–^{194}Pt–^{106}Pd-^{185}Re-enriched spike, using inverse aqua regia (2.5ml 12

mol l^{-1} HCl and 5ml 16 mol l^{-1} HNO_3) in quartz high-pressure asher (HPA) vessels. The vessels were placed in an Anton Paar HPA at Durham University at 300°C and 125 bars for at least 8 hours. The extraction and purification of Os, Ir, Ru, Pt, Pd and Re followed closely techniques described previously (Shirey and Walker, 1995; Cohen and Waters, 1996; Birck et al., 1997; Pearson and Woodland, 2000). Osmium was extracted from the inverse aqua regia using CCl_4, back-extracted using HBr, and then microdistilled. The aqua regia was dried and re-dissolved in 0.5 mol^{-1} HCl for purification of Re, Ir, Ru, Pt and Pd using AG1X-8 (100-200 mesh) anion-exchange resin.

Mineral separates. Mineral separates, hand-picked from gabbro and gabbroic eclogite samples, were optically inclusion-free, except olivine (which contains tiny opaque inclusions) and omphacite (contains exsolved rutile). The Re-Os data for olivine probably represent an upper concentration limit. Mineral separates of between 1.5 and 380 mg were cleaned in an ultrasonic bath using acetone, 2 mol l^{-1} HCl and water, dried and then powdered in agate. The procedure for dissolution and purification of Re and Os follows that of Birck et al. (1997), except that reduced volumes of reagents were used in order to minimise blanks.

Separated sulphides were processed at the Open University in either the same way as silicate separates or by microdistillation only. The latter technique involved the drying of ^{190}Os-^{185}Re-spike on the lid of a conical Teflon® vial, followed by placement of the sulphide, 25µl 12 mol l^{-1} H_2SO_4 and 20µl Cr in H_2SO_4 on the spike residue, and 15µl of 9 mol l^{-1} HBr in the apex of the vial. The vial was inverted and screwed tightly onto the lid and placed on a hotplate, resulting in full digestion, oxidation of Os and separation from Re (Pearson et al., 1998). Rhenium data for microdistilled sulphides are not presented due to considerable blank contribution.

Mass spectrometry. Whole-rock Re-Os and PGE analyses were performed at Durham University. Osmium was analysed on Pt filaments as OsO_3^- by negative-thermal ionisation mass spectrometry (N-TIMS) using the electron multiplier mode on a ThermoFinnigan Triton (after Creaser et al., 1991; Volkening et al., 1991). Repeat analyses (n=23) of 1.75 and 17 pg aliquots of the University of Maryland (College Park) Os reference material (UMd; also sometimes UMCP) at Durham University gave a $^{187}Os/^{188}Os$ mean value of 0.11378±28 (2 SD) over the time period of analysis (October 2005 – November 2007), in good agreement with a value of 0.113787±7 for much larger aliquots (>10 ng) measured on the same instrument in Faraday cup mode (Luguet et al., 2008a).

Whole-rock Re, Ir, Ru, Pt and Pd were measured by inductively-coupled plasma mass spectrometry (ICP-MS) on a ThermoFinnigan Element 2 at Durham University. Solutions were introduced using a MicroMist micro-concentric nebuliser and ESI stable sample introduction system (dual-cyclonic quartz spray chamber). Mixed solutions of natural PGE and solutions of Hf, Zr, Y and Mo (all at 1ng/g concentrations) were used to quantify the degree of mass fractionation and the production rates of HfO^+, ZrO^+, YO^+ and MoO^+ which are of equivalent mass to isotopes of Ir^+, Pt^+ and Pd^+. These solutions were analysed before, during and at the end of each analytical session.

Re-Os in mineral separates were analysed at the Open University. Osmium methodology followed that above, except for the use of the Johnson-Matthey (DTM) Os standard solution which gave a $^{187}Os/^{188}Os$ mean value of 0.17395±87 (2SD, n=18) for 0.5 and 1 pg aliquots, in good agreement with a value of 0.17394±1 for several ng Os, obtained by Birck et al. (1997). Rhenium was analysed by N-TIMS, as ReO_4^- ions.

Blanks. Total procedural blanks for Re-Os whole rock analyses (October 2005 to November 2007 were as follows (mean value in parentheses); Os: 0.04-0.51 pg (0.21) with $^{187}Os/^{188}Os$ between 0.140 and 0.675 (0.32), Ir: 0.05-1.1 pg (0.44), Ru: 0.5-4.2 pg (1.8), Pt: 1.9-5.6 pg (3.4), Pd: 3-25 pg (10), Re: 0.3-9 pg (1.6). Although the absolute values for the blank varied significantly due to reagent variability, the short-term reproducibility of the Os blank (relating to each reagent batch) was usually ±10% or better, and therefore blank corrections relate to the individual batch rather than the long-term mean. The percentage blank contribution to each analysis was always <10% for Os (and typically <2%), <30% for Ir and Ru (typically <10%), <15% for Pt (typically <5%), <38% for Pd (typically <10%) and <4% for Re (typically <2%). Blanks for mineral separates and sulphides digested at the Open University in 2004 were in the range: 0.01 - 0.36 pg Os and 0.7 - 1.6 pg Re and again, blank correction was performed according to batch (blank contribution is shown in Table 4).

Digestion efficacy, reproducibility and accuracy of HSE concentrations. HPA digestion of relatively silica-rich samples such as basalts is, as yet, not well documented. However, Re and Os whole-rock data in this study replicate data obtained from an HF-HBr dissolution (Dale et al., 2007), and illustrate that Re and Os concentrations are broadly comparable using the two techniques. In order to further assess the efficacy of Re and PGE extraction from the silicate matrix during HPA digestion, a desilicification test was undertaken on the basaltic reference materials (RM) DR26 type 1 and TDB-1, and also 2 gabbros, 1 gabbroic eclogite and 1 basaltic eclogite from this study. This involved initial dissolution in 6ml 29 mol l^{-1} HF and 2ml 12 mol l^{-1} HCl, followed by a HPA aqua regia digestion. Although the dataset is limited (Table 2), and thus susceptible to the effects of powder heterogeneity, it suggests that Pt, Pd and Re may not be fully extracted from the whole-rock powder of the two basaltic reference materials without an initial desilicification step (cf. Dale et al., 2008). However, the desilicified gabbros, gabbroic eclogite and basaltic eclogite have concentrations of Re, Pt and

Pd in good agreement with non-desilicified digestions (between 80% and 125% in all cases). Furthermore, the concentrations can be either higher, lower or essentially the same, suggesting that powder heterogeneity is the significant factor, rather than differing digestion efficacy.

Overall, duplicate digestions of the same sample powder (Table 2, n=2-4) indicate reproducibility better than 15% for Os, despite concentrations below 20 pg/g, 4-50% for Ir (one sample contains <2 pg/g Ir), 4-61% for Ru, 10-30% for Pt, <15% for Pd and <25% for Re (one analysis of S01/3iix omitted for Pt, Pd and Re), comparable to other low abundance samples (cf. Pearson and Woodland, 2000).

The accuracy of whole-rock HSE concentrations is more difficult to evaluate, but the reproducibility of data using two different digestion techniques suggests that incomplete digestion and/or sample-spike equilibration is unlikely to be a significant consideration. Data for the RM DR26 type 1 are broadly in agreement with published values (Table 2). The replicates (n = 2) of EN026 are in good agreement with each other but give lower concentrations for all PGE than published data. Meisel and Moser (2004) highlighted inter-laboratory variation for this RM which requires further study; e.g. mean Ir concentrations vary from 12 - 35 pg/g (Table 2). Data for standard HPA digestion (aqua regia, no HF) of TDB-1 lie within the range of Meisel and Moser (2004), while the desilicified analysis gave Ru, Pt, Pd and Ru values above the range of uncertainty in that study (Table 2). In summary, difficulties remain with heterogeneity in low PGE concentration RM and there is no clear evidence that one digestion method is superior to others.

In situ sulphide analysis. Sulphide HSE concentrations were measured by laser-ablation ICP-MS at the Open University, using a New Wave 213 Nd:YAG deep UV (213 nm) laser system connected to an Agilent 7500s ICP-MS. Samples were prepared as 100-200μm thick polished

sections and the major element composition was established by electron microprobe (Cameca SX100). Sulphur was used as an internal calibration for the ablation data. Ablation was performed in a pure helium atmosphere, using a 40-80 μm beam size (depending on size of sulphide) and a 10Hz laser frequency. The warm-up period was 150 seconds, the laser fired for 50 seconds, and the wash-out duration between analyses was at least 320 seconds. The data were processed in time-resolved mode using Glitter software (Van Achtebergh et al. 2001). Two 'in-house' external standards were used (initially synthesised at GEMOC, Australia); the first, PGE-A, was used for calibrating all the PGE, and the second, ReOsOA#4, was used for Re. Ruthenium masses 99 and 101 were both measured in order to assess $^{61}Ni^{40}Ar^{+}$ and $^{59}Co^{40}Ar^{+}$interferences. A strong co-variation of ^{59}Co and ^{99}Ru, and the less abundant ^{61}Ni and ^{101}Ru, was observed, suggesting significant argide interferences. Concentrations given are derived from ^{101}Ru, because this isotope yielded lower concentrations than ^{99}Ru, but the data for Ni-Co-rich sulphides could be significantly in error. Rhodium concentrations in Cu-rich sulphides also suffer an interference from $^{63}Cu^{40}Ar^{+}$ on $^{103}Rh^{+}$. A correction has been applied based on the $^{108}Pd/^{105}Pd$ ratio, which includes a $^{65}Cu^{40}Ar$ interference on ^{105}Pd, but as the uncertainty increases with the size of correction, some data have been omitted.

Sulphur. Whole-rock sulphur analyses were performed on a CS-125 LECO carbon and sulphur determinator at the University of Leicester. Each sample (1g test portion) was analysed three times, reproducibility was generally better than 4% (4 samples had poorer reproducibility at 5-10%) and detection limits were typically 10 μg/g.

4. RESULTS

4.1 Whole-rock highly siderophile element (HSE) data

4.1.1 Gabbros and Gabbroic eclogites

Gabbros display chondrite-normalised PGE-Re patterns with high palladium group-PGE/iridium group-PGE ratios (Figure 2a) (PPGE: Pd,Pt,(Rh); IPGE: Os,Ir,Ru; Barnes et al., 1985). However, they possess slightly less fractionated PGE-Re patterns than MORB, with higher Os-Ir concentrations, comparable Pt and lower Re. Two gabbro groups are apparent on the basis of Pd content: one with high Pd_N/Pt_N (>1.25) and another with lower Pd_N/Pt_N (<1.25, Figure 2a). Transitional gabbros possess essentially the same PGE patterns as their precursor gabbros (Figure 2a) although two have lower Pd/Ir (and Pd/Pt). Gabbroic eclogites display strikingly variable chondrite-normalised PGE patterns (Figure 2b) which, for the most part, are fractionated with high PPGE/IPGE ratios (and high Re/IPGE), but Pt, Pd and possibly Ru concentrations appear to differ from the unaltered gabbros.

Figure 2 here.

All PGE concentrations in the gabbros vary by approximately two orders of magnitude (Table 2). Gabbroic Os concentrations display a larger range than gabbroic eclogites (2.3 to 321 pg/g and 1.6 to 105 pg/g, respectively), largely due to one PGE-rich gabbro. The ranges of Pt and Re are broadly comparable (Table 2), while the gabbro Ru range is somewhat larger (<10 to 581 pg/g) than the gabbroic eclogites (<6 to 95 pg/g). Palladium concentrations display the greatest difference, with gabbros varying from 13 to 1780 pg/g and gabbroic eclogites only from 19 to 176 pg/g.

The mean values for the gabbro and gabbroic eclogite suites are different (e.g. 64 and 31 pg/g Os respectively, Table 2). However, by omitting the one particularly PGE-rich gabbro, the

protoliths and their metamorphosed equivalents have indistinguishable mean concentrations: Os - 27 and 31 pg/g, respectively, Ir - 19 and 24 pg/g, Ru - 41 and 41 pg/g and Pt - 243 and 243 pg/g (in each case 1 standard deviation is approximately equal to the mean itself). Mean Re content differs slightly and is about 20% lower in the gabbros. Re-Os isotope data do not permit significant loss or gain of Re or Os, unless shortly after igneous crystallisation (Dale et al., 2007), and are therefore consistent with the similar mean concentrations derived from omitting the PGE-rich gabbro. Given the low concentrations and heterogeneous distribution of the PGE, coupled with an episode of metamorphism, the similarity in mean abundances is remarkable.

In contrast to Pt, Re and the IPGE, mean Pd concentrations are markedly different in the gabbroic and eclogitic suites (355 pg/g and 80 pg/g, respectively, Table 2 and Figure 2). Assuming similar initial igneous concentrations of Pd, as with the other PGE, this equates to Pd loss of ~75% (Figure 3). Lower Pd_{mean}/Ir_{mean} in the eclogites (3.4 compared to 18.4) and typically lower Pd_N/Pt_N ratios (0.1 to 2.6 compared to 0.9 to 4.1), are also consistent with Pd loss.

MgO – PGE systematics. Abundances of PGE and Re in the gabbros co-vary positively with MgO content (e.g. Figure EA-1, electronic annex), with r^2 fits of 0.6 to 0.8. Chondrite-normalised Os/Ir ratios (Os_N/Ir_N) for the gabbros range from 1.0 to 1.7, with a mean of 1.4, and display no co-variation with MgO between 14 and 6.5 wt. % (Figure 4). Despite more Os_N/Ir_N variability in the gabbroic eclogites, the mean of 1.3 is indistinguishable from the gabbros. With one exception (namely the highest MgO sample) the gabbros define a positive array between Ru_N/Ir_N and MgO, while gabbroic eclogites scatter to both higher and lower ratios.

Figure 3 here.

Pt_N/Ir_N ratios in gabbros may increase and then decrease with decreasing MgO (Figure 4). Gabbroic eclogites display considerable Pt_N/Ir_N variation for a given MgO content and have a greater range of Pt_N/Ir_N ratios, extending both higher and lower than the gabbros (1.2 - 33.5 and 1.8 - 8.9, respectively). Gabbros with Pd_N/Pt_N >1.25 define a negative co-variation in MgO - Pd_N/Ir_N space (r^2 – 0.97), whereas other gabbros plot below this array, towards a cluster of gabbroic eclogites, which have significantly lower Pd_N/Ir_N.

Table 2 here.

Figure 4 here.

4.1.2 Basaltic eclogites

The variation in basaltic eclogite 'common' Os concentrations (after subtraction of in-grown ^{187}Os) is fairly small, from 2.7 to 12 pg/g (Table 2), with a mean of 8.1 pg/g, similar to MORB (~9 pg/g, Schiano et al., 1997; Escrig et al., 2004; Escrig et al., 2005; Gannoun et al., 2007). Ruthenium concentrations (16 – 35 pg/g, mean: 26) are slightly lower than mean MORB (47 pg/g, Rehkämper et al., 1999; Bezos et al., 2005).

The most striking aspect of basaltic eclogite PGE data is their extremely low Pd concentrations relative to MORB (Table 2, Figures 4 and 5). The mean Pd concentration of 55 pg/g equates to a loss of ~90% when compared to ~660 pg/g for MORB (Rehkämper et al., 1999; Bezos et al., 2005), and even accounting for substantial uncertainty in the MORB average suggests loss of at least 85% (e.g. if MORB mean = 400 pg/g). Rhenium concentrations are much lower than in MORB (398 pg/g and 1100 pg/g, respectively (Sun et al., 2003; Gannoun et al., 2007)), suggesting ~60% loss, consistent with a previous study of these rocks (Dale et al., 2007) and another study of metabasalts (Becker, 2000). The mean Pt abundance of the metabasalts (112 pg/g) is also considerably lower than the MORB average

(~340 pg/g, Rehkämper et al., 1999; Bezos et al., 2005) despite one analysis with a fairly high Pt concentration (437 pg/g). The other basaltic eclogites have a mean Pt content of only 47 pg/g, and mostly have Pt/Ir ratios that are at the low end of the MORB range (Figure 4). Pt depletion in these rocks may be ≥60% on average, or ≥160 pg/g in actual terms, even when including the Pt-rich sample. Thus, basaltic eclogites have much flatter chondrite-normalised PGE patterns than typical MORB samples with significantly lower PPGE/IPGE (Figure 5).

Figure 5 here.

4.2 HSE abundances in gabbroic and eclogitic sulphides

Gabbro-hosted sulphides. Pyrrhotite displays relatively unfractionated PGE patterns with Pd_N/Ir_N of 0.2 to 6 (lowest in S01/36ix) and Re_N/Os_N of 1 to 9. However, Pt is fractionated from the other PGE and is present at exceptionally low normalised concentrations compared to Pd and Rh (Figure 6). This has previously been observed in mantle sulphides (Alard et al., 2000; Luguet et al., 2001; Lorand et al., 2008) where Pt is found to be concentrated in associated alloys, rather than being abundant in the sulphide itself. These Pt-rich alloys have been identified by discrete Pt spikes in the laser-ablation time-resolved spectrum in one of the gabbros analysed. Pentlandite also possesses low Pt concentrations, but has much higher Pd and somewhat higher Re, Rh and Ag (Figures 6 & 7 and Table 3). Chalcopyrite is enriched in Pd, Re, Ru, Ag and Pt, relative to pyrrhotite. Both pentlandite and chalcopyrite have slightly lower Os and Ir content than pyrrhotite and greater Re/Os ratios.

Figure 6 here.

Osmium concentrations in gabbro-hosted sulphides are heterogeneous and vary by up to 2 orders of magnitude, with a typical range of <0.003 to 0.07 μg/g (Table 3, mean: 0.043 μg/g). Rhenium concentrations are similarly heterogeneous and typically vary from 0.002 to 0.09

μg/g in all samples analysed (mean: ~0.014 μg/g). Almost all gabbro-hosted sulphides have Re/Os <1 (Figures 7 and 9), and mean Re/Os ratios are 0.29, 0.32 and 0.44 for the 3 different gabbros. Such Re concentrations and Re/Os ratios are considerably lower than the available data for MORB sulphides (0.069 to 3.2 μg/g and typically >1, Roy-Barman et al., 1998; Gannoun et al., 2004). Gabbroic sulphides have Pt abundances of <0.002 to 0.06 μg/g (Table 3), much lower than a published MORB sulphide (~30 μg/g, Peach et al., 1990), but as the latter was a bulk sulphide analysis (RNAA) it may have included associated Pt-rich micro-phases. Ruthenium tends to be significantly more abundant than Os and Ir, with a concentration range of at least <0.05 to 0.17 μg/g; argide interferences precluded accurate determination of Ru in pentlandite, but Ru has been shown to be compatible in this phase (Makovicky et al., 1985).

Palladium concentrations span nearly three orders of magnitude and, unlike the other PGE and Re, co-vary positively with sulphide Ni abundance (Figure 8), and to a lesser extent with Cu. This co-variation is particularly well-defined in two gabbros (r^2 = 0.83 and 0.98), which define two arrays with similar slopes but different absolute abundances, consistent with their different whole-rock Pd abundances. In contrast, eclogitic sulphides do not display co-variation of Pd and Ni and have a limited range of Ni content. Platinum does not co-vary with Ni in either gabbroic or eclogitic sulphides (Figure 8b), but it does display weak positive co-variation with Cu in some samples.

Table 3 here.

Figure 7 here.

Gabbroic eclogite-hosted sulphides. Unlike the sulphide assemblage in gabbros, pyrite is present and predominant in gabbroic eclogites, and pentlandite is absent. Pyrites from all

three eclogites have similar PGE-Re patterns and, compared to all gabbroic sulphide types, most have lower Os, Ru and Ir concentrations and very variable Pt contents (Figures 6 & 7 and Table 3). They also have higher Re concentrations and Re/Os ratios (0.04 to 69) than gabbroic sulphides (typically 0.04 to 4, e.g. Figure 10). All but one eclogite-hosted sulphide (Py, Po, Cp) has an Os/Ir ratio greater than unity. One gabbroic eclogite hosts a distinct pyrite group (group II in Figure 6) which has high Os-Ir concentrations, relatively high Pt, low Ru/Ir and very low Pd/Ir ratios. Cobalt contents of this group are higher than group I pyrites from the same sample, but within the range of all eclogitic pyrites analysed. Overall, the range of PGE concentrations in pyrites is broadly comparable to that of gabbroic sulphides, with the exception of Pd which is less concentrated in pyrite than in almost all gabbroic sulphides (Figure 7).

Figure 8 here.

4.3 Re-Os abundances in silicate and oxide mineral separates

4.3.1 Gabbroic minerals

Figure 9 illustrates broad co-variance of Re and Os in gabbroic silicates, oxides and sulphides. Plagioclase and the most inclusion-free olivine possess the most extreme Re/Os ratios observed in silicates and oxides (>350 and 3.7, respectively, Table 4). As expected for highly siderophile and chalcophile elements, Re and Os abundances in silicate phases are low and range from <0.5 pg/g in plagioclase, through augite (1-3 pg/g), and are highest in olivine (6-19 pg/g). A mixed ilmenite/chromite fraction contains ~130 pg/g Os, around ten times the whole-rock content.

Figure 9 here.

Rhenium concentrations in silicate and oxide phases are considerably higher than Os, perhaps due to a different charge and ionic radius of Re in melts (cf. Ertel et al., 2001). Concentrations in olivine range from 24 to ~710 pg/g in two separates from the same sample (Table 4). Such a disparity is almost certainly due to the unavoidable sampling of Re-rich inclusions, most likely sulphide but also probably chromite. Plagioclase and augite contain Re at a concentration broadly comparable to the whole-rock (~170, ~120 and ~162 pg/g, respectively). The Al-chromite + ilmenite fraction has relatively abundant Re (~1130 pg/g).

4.3.2 Gabbroic eclogite minerals

Os concentrations are less variable in eclogite phases (5 to 150 pg/g, Table 4) than gabbro phases. Saussurite, the micro-crystalline multi-phase product of HP plagioclase breakdown, possesses the lowest Os abundances, consistent with the low Os abundance of the precursor phase. Coarse omphacite containing some rutile inclusions, likely formed in igneous pyroxene domains, has Os concentrations of 13 and 33 pg/g in the two separates analysed. Glaucophane and talc from the Os-rich eclogite S01/3iix both have surprisingly high Os contents (90 and 150 pg/g, respectively) that may, in part, reflect inheritance of much of their chemistry from the precursor olivine igneous domain containing numerous relatively Os-rich sulphide and chromite inclusions.

Garnet contains by far the highest Re abundances (~1000 and ~7000 pg/g in two different eclogites, Table 4). Saussurite, like its precursor plagioclase, contains ~75-140 pg/g Re. Omphacite in one eclogite contains ~300 pg/g Re. Given that talc and glaucophane formed in the same domain, it is evident that Re is preferentially incorporated into talc (600 and 350 pg/g) rather than glaucophane (~130 pg/g).

Table 4 here.

4.4 Re-Os isotope data for minerals

Whole-rock Re-Os data for Allalin gabbros and gabbroic eclogites presented in Dale et al. (2007) give model ages and an errorchron age in broad agreement with the age of igneous crystallization (164 Ma, Rubatto et al., 1998), demonstrating that the Re-Os system has not been significantly disturbed during high-pressure metamorphism.

Gabbros. Whole-rock, olivine, augite and sulphide Re-Os measurements for S01/39iiix give model ages which are close to the age of igneous crystallisation (Figure 10). This indicates that even on a mineral-scale the Re-Os system remained largely 'closed' within unrecrystallised samples, despite these rocks being subject to P-T conditions of 600°C and >2 GPa. However, an ilmenite and Al-chromite separate and a sulphide grain do yield young model ages suggesting that the Re-Os system has locally been disturbed at the mineral scale during metamorphism. Inclusion-rich olivine and augite from another gabbro (S02/83vix) also have model ages broadly consistent with the age of igneous crystallisation (146 and 195 Ma, Figure 10).

Figure 10 here.

Gabbroic eclogites. By using an initial composition derived from the whole-rock at 45 Ma ($^{187}Os/^{188}Os$ ~0.17), model ages close to the timing of peak metamorphism are generated (Figure 10). The ages scatter considerably, but most of the phases measured yield ages within uncertainty of the time of the peak of high-pressure metamorphism (ca. 45 Ma). These data clearly indicate that the eclogitic minerals, both silicate and sulphide, relate to crystallisation or equilibration at the time of HP metamorphism. In this case, the distribution of HSE must also largely relate to the same HP metamorphism rather than some earlier event.

5. DISCUSSION

5.1 HSE systematics in whole-rock gabbros

In comparison with MORB, the relatively MgO-rich cumulate gabbros have less fractionated PGE patterns (lower PPGE/IPGE, Figure 2a). The IPGE are present in higher concentrations than in MORB, whereas Pt and Pd concentrations are similar and Re contents are lower. The relative compatibility of the PGE during fractional crystallisation in mid-ocean ridge systems, can be inferred by comparison of gabbro and MORB and is similar to that during mantle melting: i.e. Os≈Ir≥Ru>Pt>Pd>Re (e.g. Keays et al., 1981; Barnes et al., 1985). Thus, fractionation of the phases present in the cumulate gabbros (primarily olivine + plagioclase, but with associated sulphides and oxides) is likely to drive melts to increased PPGE/IPGE ratios. This observation can, in part, explain the generation of very high PPGE/IPGE ratios found in MORB (cf. Rehkämper et al., 1999; Tatsumi et al., 1999; Bezos et al., 2005), although significant fractionation of the PPGE and IPGE is still required during mantle melting.

The two gabbro groups, defined by Pd_N/Pt_N ratios (>1.25 and <1.25, Figure 2a), could be generated either by an igneous or post-igneous process. Magmatic variations in the modal proportion of different sulphide phases may account for such a difference, but the proportion of pyrrhotite, pentlandite and chalcopyrite does not seem to significantly vary between the groups. Furthermore, Pd_N/Ir_N variation is decoupled from differentiation indices such as MgO (Figure 4) and Ni, thus suggesting a post-igneous origin for the two groups. Gabbros with Pd_N/Pt_N >1.25 define a negative co-variation in MgO - Pd_N/Ir_N space ($r^2 = 0.97$), which likely represents the original magmatic array, whereas gabbros with Pd_N/Pt_N <1.25 plot below this array, towards the low Pd/Ir gabbroic eclogites, most likely due to minor Pd loss during alteration and/or metamorphism. Clearly the estimated degree of Pd loss between gabbroic

protolith and eclogite (>75%, Figure 3) depends on the origin of the Pd/Pt variation and if some gabbros have experienced post-magmatic Pd loss then the true degree of loss from pristine gabbro to gabbroic eclogite could be greater than estimated here.

There is clear positive co-variance between all the PGE (e.g. Figure EA-2). Os, Ir and Ru display particularly well-defined arrays ($r^2 = 0.99$), but there is also positive co-variance of Os with Pd and Pt ($r^2 = 0.63$ and 0.86, respectively). Rhenium-PGE co-variance is less clearly defined, but is stronger with the PPGE than the IPGE. All whole-rock PGE abundances decrease with decreasing MgO and sulphur content, in accord with extraction of immiscible sulphide during fractional crystallisation due to sulphur-saturation of the magma (cf. Puchtel and Humayun, 2000; Bezos et al., 2005), and the high sulphide-silicate melt partition coefficients of the PGE (e.g. Peach et al., 1990). A comparison of PGE/Ir, Pd/Pt and Pt/Re ratios with S content (not shown), suggests the relative order of PGE compatibility in the gabbroic sulphides: Ir>Ru≈Os>Pd>Pt>Re (consistent with sulphide data in this study, except Ir) or alternatively could suggest that sulphur content is driven by other changes in the proportions of accumulating phases which instead control the PGE ratio variations. Similar co-variation of PGE/Ir ratios and Cr abundance suggests that chromite could also play a significant role in the fractionation of PGE through the nucleation of Os-Ir-Ru alloys, as proposed by Ballhaus et al. (2006). However, the gabbroic whole-rock budgets of the IPGE appear to be dominated by sulphide (section 4.5) and thus the variations reflect co-variation of S and Cr, rather than control by chromite. Crystallisation of chromite would reduce FeO in the melt, thus inducing sulphide precipitation (e.g. O'Neill and Mavrogenes, 2002).

Based on the slopes of the MgO-PGE/Ir arrays (Figure 4), and MgO-Pd/Pt, it can be inferred that the relative bulk-rock PGE partition coefficients decrease in the following order: Ru>Ir≈Os>Pt>Pd>Re. For instance, the positive array between Ru_N/Ir_N and MgO (6 to 14 wt.

%) in the gabbros suggests greater compatibility of Ru over Ir in the higher MgO assemblages, which are also more S-rich (Table 2) due to greater sulphide precipitation associated with olivine +/- chromite crystallisation. This order of relative bulk partitioning differs slightly from that derived from PGE-sulphur systematics in that Ru appears to be the most compatible on a bulk-rock scale. The greater bulk compatibility of Ru may be explained by the positive co-variation of Ru/Os (and Ru/Ir) with modal proportion of olivine (Figure EA-3), suggesting that Ru is more compatible (than Ir or Os) in this phase, although previous experimental studies (Brenan et al., 2003; 2005) imply very similar olivine/melt partitioning for Ru and Ir. Spinel and Fe-oxides, both present in the gabbros (Al-chromite and ilmenite), have also been proposed as significant hosts of Ru (Capobianco and Drake, 1990; Capobianco et al., 1994), but co-variation of Ru/Ir and the modal proportion of oxides is not observed in these gabbros. Palladium is inferred to be more compatible than Pt in sulphide, but not in the bulk-rock, consistent with Pt being hosted by other phases (Figure 12) and also reflecting the extremely chalcophile nature of Pd (e.g. Peach et al., 1990).

It is possible that inflected, rather than straight, best-fit lines can be drawn through the MgO-PGE/Ir data (Figure 4), although the inflection is largely based on one Mg-rich sample. Such an inflection, if real, would indicate a change in bulk partitioning possibly due to a change in the type of sulphide precipitated, or the cessation of chromite and/or associated PGE-rich micro-phase crystallisation.

The inferred greater bulk compatibility of Ru over Ir in relatively Mg-rich samples (6 - 14 wt. % MgO), is at odds with the observation that basalts, whose parental magmas have presumably undergone significant fractional crystallisation of olivine, have higher chondrite-normalised Ru contents than Os or Ir. However, this in part may be reconciled by the

generation of elevated Ru/Ir during partial melting and possibly by a change in partitioning behaviour with MgO content, as suggested above.

Gabbroic Os_N/Ir_N ratios are greater than unity and are therefore higher than most mantle rocks which contain roughly chondritic proportions of Os and Ir as a result of little fractionation between these elements during mantle melting (Lorand et al., 1999; Pearson et al., 2004). The chondritic Os/Ir ratio of the Mg-rich gabbro S02/6ix suggests that Os-Ir fractionation may occur during early fractional crystallization (possibly due to sulphide precipitation or micro-alloy formation), resulting in higher, and broadly constant, Os_N/Ir_N in lower MgO samples (Figure 4).

5.2 Whole-rock and mineral-scale HSE variations accompanying eclogite formation

5.2.1 Whole-rock HSE variations accompanying eclogitisation

The mean abundances of the PGE in gabbros and gabbroic eclogites suggest that significant fractional loss of Pd has occurred during metamorphism, equating to approximately 75% of the original igneous concentration (or greater if some gabbros also record Pd loss). No other PGE or Re appears to have been significantly depleted or enriched during metamorphism (Figure 3). Mean concentrations of Re, Os and Ir are slightly higher in the gabbroic eclogite suite than in the gabbros (if the anomalous PGE-rich gabbro, S02/6ix, is omitted). However, these differences are not significant given the heterogeneous distribution of the PGE and the relatively small sample set. Moreover, Re and Os are known, on the basis of isotope evidence, not to have been significantly enriched or depleted in these samples during metamorphism (Dale et al., 2007). Platinum has clearly been mobilised during metamorphism (as illustrated by the highly variable Pt/Ir ratios of gabbroic eclogites), but the degree of, or distance over which, this mobilisation has occurred was probably relatively

limited given that the mean Pt abundances of the gabbros and eclogites are essentially identical.

In contrast, the basaltic eclogites display considerable depletion of Pt (≥60%), Pd (>85%) and Re (50-60%, this study, Dale et al., 2007), relative to MORB (Figure 3). Rhenium loss of ~60% has also been found in a study of other basaltic eclogites (Becker, 2000). The depletion of Re is significantly less in percentage terms than that of Pd, but in absolute terms each sample has lost, on average, ~600 pg/g Re, ≥350 pg/g Pd and ≥160 pg/g Pt. Some mobility of Os, Ir or Ru cannot be ruled out as the means for basaltic eclogites are lower than mean MORB (Os: -10%, Ir: -30%, Ru -45%), but at such low concentrations any estimate carries considerable uncertainties.

As the temperature of metamorphism (~600°C) was insufficient to induce melting of hydrous basalt or gabbro, it seems likely that Pd, Pt and Re were mobilised in a high-pressure fluid. Gammons and Bloom (1993) and Wood et al. (1992) both found Pt and Pd to be soluble in sulphur-bearing fluids, complexed with HS, although only the former concluded that Pd is more soluble than Pt. The loss of Pd from both basaltic and gabbroic lithologies suggests that this element is the most susceptible to release and mobility in a fluid. The observed loss of Pt and Re from basaltic samples probably primarily results from a greater degree of hydration and deformation than occurred in the gabbros. Deeply emplaced and massive gabbroic bodies are likely to experience more limited hydrothermal and low-temperature seafloor alteration. Thus, as a consequence of this limited alteration and their different rheological properties, they will be less easily deformed during subduction.

5.2.2 Distribution of HSE within a gabbro and a gabbroic eclogite

Rhenium and Os concentrations in all the major constituent phases of a gabbro and a gabbroic eclogite, combined from separated and in situ analyses (Tables 3 and 4), can be taken with the estimated modal proportions of silicate and sulphide in order to calculate the contribution of each phase to the whole rock budget of these elements. The in situ sulphide PGE data (Table 3) may also be combined with sulphur abundance to estimate the proportion of whole-rock Os, Ir, Ru, Pt, Pd and Re accounted for by sulphide in the gabbros and gabbroic eclogites.

On the basis of electron probe micro-analysis (Table 1) and the sulphide phase modal proportions, sulphide was taken to contain 36.5% S in the gabbroic samples and 47.5% S in the eclogites. This was then combined with the sulphur concentration to calculate sulphide abundance. It is important to note that calculated phase contributions to the Re and Os whole-rock budget are poorly constrained due to uncertainties in estimating the modal proportions of sulphide and silicate phases, the lack of replicate analyses of many phases, and limited laser-ablation sampling of sulphide grains which have highly variable PGE abundances. Despite such uncertainties, these data provide, for the first time, a quantitative estimate of the proportion of HSE in silicate and sulphide phases from a gabbro and its metamorphosed equivalent.

Rhenium-osmium. Approximately 90% of the whole rock abundance of Os in the gabbro S01/39iiix can be accounted for by sulphide (Figure 11). Olivine and the oxide fraction (chromite/ilmenite) together contain ~10% of the budget, but the olivine, while hand-picked, unavoidably contained some sulphide and oxide inclusions so the percentage of Os in pure olivine will almost certainly be lower still. By contrast, sulphide contains only ~5% of the whole-rock Re. Plagioclase accounts for the majority of the Re budget (75-80%), while augite contains <10% of the Re due to its much lower modal abundance. Oxides contain high

Re concentrations (1130 pg/g) but only account for a minor proportion of the whole-rock (~5%) due to their low modal abundance.

Figure 11 here.

In the gabbroic eclogite S01/3iix, sulphide dominates the whole-rock budget of Os (~70%, Figure 11). Glaucophane and talc, which crystallised within the olivine domain, account for most of the remainder of the budget, probably due to inheritance of Os from the many tiny sulphide inclusions originally within olivine. Garnet probably hosts the majority of Re, while saussurite, the product of HP plagioclase breakdown, can also account for a significant proportion.

HSE in sulphides. Gabbro-hosted sulphides (Po, Pn, Cp) account, on average, for >70% of the whole-rock Os, Ir and Ru budget (Figure 12a). In two of the samples, sulphide accommodates ~100% of the budget of these elements, whereas in the third, PGE-rich gabbro, less than 30% of the IPGE can be accounted for by sulphide. The low proportion of PGE in sulphides from this sample may be explained by the presence of tiny early-formed sulphide inclusions in olivine, too small to be analysed, which are presumably PGE-rich compared to later-precipitated inter-granular sulphides. Palladium is also largely hosted by sulphide, particularly in the two PGE-poorer samples (~80%, mean: ~60%). The contribution of sulphide to the whole-rock content of Pt and Re is very low; ~5% in both cases.

Despite large variations in the fraction of PGE accounted for by sulphide in the different gabbroic eclogites, the mean percentage of whole-rock Os, Ir and Ru in gabbroic eclogite-hosted sulphides (Py, Po, Cp) is significantly lower than in the gabbros (~50%, Figure 12b). Platinum appears to be present in greater concentrations in the pyrite lattice than in gabbroic sulphides (Figures 6 & 7), where it was probably concentrated in associated alloys, and hence

sulphide may account for as much as 30% of the eclogite whole-rock budget. Due to considerably lower Pd concentrations, eclogitic sulphides can only account for about 40% of the budget, despite much lower whole-rock Pd contents. The proportion of Re hosted by sulphide is greater than in gabbroic sulphides but is still only ~15% of the whole-rock content.

Figure 12 here.

Basaltic sulphides, not included in this study, may possess different average PGE concentrations to those in gabbros due to variation in sulphide type. With decreasing MgO driven by fractional crystallisation, sulphide precipitation will change from predominantly iron-rich to more copper-rich varieties (Czamanske and Moore, 1977). The latter are preferred by the chalcophile Re and Pd (e.g. this study), resulting in higher Re/Os ratios in MORB sulphides (cf. Gannoun et al., 2004). However, MORB sulphides still consist primarily of mss/pyrrhotite, pentlandite and iss/chalcopyrite (Czamanske and Moore, 1977) and hence it is reasonable to apply some of the findings from the gabbroic eclogites to the interpretation of the basaltic eclogites.

5.2.3 Mineral-scale evidence for the redistribution and loss of HSE during metamorphism

The mean sulphur content of the gabbroic eclogites is 401 μg/g (n = 8), ~15-20% lower than the gabbros (494 μg/g, n=8), perhaps suggesting a reduction in sulphur content between igneous crystallisation and exhumation (although the data vary such that the two suites are indistinguishable within uncertainty). Furthermore, there has been a predominant phase change from igneous pyrrhotite + pentlandite (+ minor chalcopyrite) to more sulphur-rich pyrite in the gabbroic eclogites (with subsidiary pyrrhotite and minor chalcopyrite). The phase change marks coincident loss of nickel (and probably copper) from sulphide and indicates evolution towards decreasing metal/S ratios in sulphide during metamorphism

(Table 1). Thus, the modal abundance of sulphide in the gabbroic eclogites has decreased by a greater degree than S content from, on average, 0.135% in the gabbros to 0.084% in the eclogites (38% reduction). The average sulphur content of the basaltic eclogites is ~1100 ug/g, which is within the range observed for MORB (1000 to 1800 Mathez, 1976). Thus, it is not possible to ascertain whether the basalts have lost a significant proportion of sulphide, but as with the gabbroic eclogites, sulphur appears to have been mobilised, modified and now forms large grains predominantly composed of pyrite.

The whole-rock Pd budget is largely controlled by sulphide, and the highest Pd concentrations are found in pentlandite (Figure 6, 7 & 8, section 4.2). Thus, the transformation from a gabbroic sulphide assemblage of largely pyrrhotite + pentlandite to pyrite + pyrrhotite in eclogites provides a mechanism for the release and loss of Pd from the whole-rock. In contrast, Pt contents in eclogitic sulphides are typically higher than those in gabbros (Figure 7), and the proportion of whole-rock Pt hosted by eclogitic sulphides is greater (Figure 12). This suggests that the Pt-rich micro-phases associated with the igneous sulphides may, at least in part, have broken-down during metamorphism and, moreover, that much of this Pt has been incorporated into the newly formed pyrite, rather than being mobilised on a larger scale. Although no PGE data for basaltic eclogite sulphides are presented, the predominance of pyrite and absence of Ni-rich sulphide, compared to sulphide globules in primitive MORB glasses (Czamanske and Moore, 1977), is likely to account for much of the depletion of Pd. However, in the case of the basalts, Pt is also clearly depleted. This difference in Pt mobility could be due to greater deformation and fluid flow in the basalts, or possibly due to greater retention of Pt in micro-phases in gabbros.

Transitional gabbros only display minor Pd depletion despite petrographical evidence for the mobilisation of sulphide. However, there is little change in sulphide composition compared

to the gabbros (i.e. pyrrhotite > pentlandite > chalcopyrite). This is again consistent with the majority of Pd loss being linked to changes in sulphide composition. Such evidence could be taken as indicative of a difference in process (i.e. no Pd loss, therefore the loss is a result of HP metamorphism) or a difference of degree (i.e. there is no Pd loss because the degree of hydrothermal alteration was not as great as for the completely recrystallised eclogites). It is, therefore, difficult to be certain that pyrite formation and loss of Pd is not the result of hydrothermal activity. However, the absence of euhedral single phase pyrite crystals and the fact that there is no increase in sulphur content in the gabbroic eclogites is strong evidence for a metamorphic origin (Lorand and Juteau, 2000; Luguet et al., 2004). In any event, the Re-Os model ages for sulphides (Figure 10) indicate recrystallisation or diffusional equilibration of sulphide during HP metamorphism, probably with concurrent Pd loss.

The lack of whole-rock depletion of Os, Ir and Ru in gabbroic eclogites (Figure 3), despite sulphides hosting a lower proportion of the whole-rock budget (Figure 12), requires Os, Ir and Ru to be incorporated into silicate and/or alloy phases during metamorphism. The high Os content of talc and glaucophane in the gabbroic eclogite S01/3iix (~90 and 150 pg/g, respectively, Table 4) can largely account for the Os lost from sulphide. These concentrations probably reflect inheritance from the precursor sulphide- and oxide-rich igneous olivine site, rather than preferential partitioning into these phases. This inheritance suggests immobility of Os in the fluid phase while the lack of whole-rock depletion also illustrates a lack of large-scale mobilisation of Os, Ir or Ru. Whether Os is hosted in the lattice of amphibole or talc, or whether they form tiny discrete PGE-rich micro-phases, cannot be determined.

The depletion of Re observed in the metabasalts (Figure 5) cannot be linked to the transformation of sulphide mineralogy, due to the small contribution made by sulphides to the whole-rock budget (Figures 11 & 12). Rhenium in gabbros is largely hosted in silicates

(plagioclase in particular). Although basaltic sulphides may contain greater abundances of Re than those in gabbros (due to a greater proportion of Re-rich Cu-sulphides), the whole-rock Re budget of basalts is also known to be largely hosted by silicates (Gannoun et al., 2004). Despite evidence for strong Re partitioning into garnet in gabbroic eclogites (Figure 11, Table 4), this is clearly not a mechanism by which Re can be retained in basaltic crust, given the apparent degree of Re depletion.

5.3 Implications for recycling, sub-arc metasomatism and the source of super-chondritic ^{187}Os and ^{186}Os compositions in OIB

Slab flux and sub-arc metasomatism. The Re-Os isotope data of this and a previous study indicate that the Re-Os system has remained 'closed' in ZSO gabbroic eclogites, and therefore gabbro-derived fluids may not contain significant Re or Os (Dale et al., 2007). However, the data from the basaltic portion of metamorphosed crust suggest a significant Re flux into the sub-arc mantle (Figures 3 & 5). The Os elemental data for metabasalts are inconclusive, although significant depletion seems unlikely. Some studies have concluded that Os is transferred to the sub-arc mantle in significant quantities (e.g. Brandon et al., 1996; Borg et al., 2000; Widom et al., 2003) while others have found no evidence of radiogenic Os transfer (e.g. Chesley et al., 2002; Walker et al., 2002; Woodland et al., 2002). However, it has been suggested that the mobility of Os in slab-derived fluids may depend on oxygen fugacity and chlorine content (Brandon et al., 1996).

Subducting oceanic crust is likely to generate a significant flux of the PPGE into the sub-arc mantle, with Pt derived from basaltic crust and Pd from both gabbroic and basaltic crust, while the IPGE appear not to be significantly depleted in either metamorphosed gabbro or basalt (Figure 13). Whether such a flux of Pt and Pd generates a noticeable enrichment in the mantle perhaps depends on the degree of prior depletion of the mantle wedge (which would

reduce Pd and Pt concentrations) and also on fluid-rock ratios and whether there is a mechanism for further enrichment or concentration of the PGE in the fluid phase, perhaps through the stripping of PGE from peridotite. Regardless of the precise mechanism, high-degree enrichments of Pd and Pt, relative to the IPGE, have been previously identified in sub-arc mantle (McInnes et al., 1999; Kepezhinskas et al., 2002; Lee, 2002).

Figure 13 here.

The source of ^{187}Os-^{186}Os enrichment. The coupled enrichment of ^{187}Os (derived from ^{187}Re decay) and ^{186}Os (from decay of ^{190}Pt), found most notably in Hawaiian picrites, has been explained by a contribution from the outer core to mantle plume sources (Brandon et al., 1999; Puchtel et al., 2005), while others have suggested possible explanations via recycling of oceanic crust. Platinum abundances in the gabbros of this study are comparable to MORB (~360 and ~340 pg/g, respectively), although gabbros that have passed through subduction zones may retain higher concentrations of Pt than basalts, due to significant loss from the latter (>60%, this study). However, irrespective of whether Pt is lost from the subducting slab, Pt concentrations, and critically Pt/Re ratios, are not sufficiently high in basaltic or gabbroic crust to generate the most radiogenic ^{186}Os/^{188}Os ratios or the coupled ^{186}Os-^{187}Os enrichments found in OIB. Approximately 97% recycled oceanic crust contribution is required for the highest ^{186}Os/^{188}Os Hawaiian picrite, even if the crust was 2.5 Ga, while at these proportions ^{187}Os/^{188}Os would be much higher than observed (>1). Recently it has been proposed that coupled radiogenic ^{186}Os/^{188}Os and ^{187}Os/^{188}Os ratios in OIB could be generated by metasomatic sulphide in the mantle source, potentially emplaced by melt percolation derived from pyroxenite or peridotite (Luguet et al., 2008b). The loss of Pt and Re from basaltic crust (documented in this study) and their likely transfer into the mantle wedge by slab fluids, provides an alternative and globally widespread mechanism for the

generation of Pt- and Re-enriched material. Platinum concentrations in the oceanic crust are low in comparison to mantle peridotite, but the large volume of continually subducting crust could provide a major Pt flux. However, modelling of mantle enriched in this way suggests that addition of slab-derived Re and Pt would not generate the observed ^{186}Os-^{187}Os enrichments, due to low Pt/Re ratios. Thus, this mechanism would probably require further scavenging of Pt from the overriding mantle wedge or the oceanic lithosphere, and/or preferential enrichment of Pt in metasomatic sulphide.

6. CONCLUDING REMARKS

The results presented here allow (i) quantification of the contribution of mineral phases to the whole-rock PGE and Re abundances of gabbroic oceanic crust and the budget of the gabbroic crust as a whole, and (ii) an assessment of the effects of subduction-related metamorphism on whole-rock and mineral PGE abundances and distribution, and the implications for fluxes into arc mantle and the PGE budget of recycled oceanic crust.

Gabbros possess chondrite-normalised PGE-Re patterns which are similar in shape and concentration to mid-ocean ridge basalts, with high Pt-Pd-Re relative to Os-Ir-Ru. However, they have slightly higher IPGE concentrations, consistent with their more primitive nature and the relative compatibility of the PGE (Ir≈Os>Ru>Pt>Pd>Re).

Rhenium and Os abundances in gabbroic silicates, oxides and sulphides reveal that the Os budget is almost entirely controlled by sulphide (particularly pyrrhotite). Rhenium, however, is hosted mainly in silicates, particularly plagioclase (~75% in one sample) due to its moderately high Re concentration (170 pg/g) and high modal abundance. Sulphide accounts for <10% of whole-rock Re. Iridium, Ru and Pd are all predominantly hosted in sulphide (typically >80% of the whole-rock budget), whereas chondrite-normalised Pt concentrations

are typically much lower than other PGE and only account for ~5% of the whole-rock budget. Pt-rich micro-phases have been identified and probably significantly contribute to the budget.

Gabbroic eclogites, by comparison with their precursor gabbros, appear to be strongly depleted in Pd (~75% loss). There is no evidence for significant loss of the other PGE or Re. Platinum has been mobilised to a degree, as indicated by variable Pt/Ir ratios in gabbroic eclogites, but the mean concentration is essentially identical to that of the gabbros. In contrast, basaltic eclogites have significantly lower Pd, Pt and Re concentrations and lower Pd-PGE/Ir-PGE ratios than mean MORB, suggesting losses of >85%, ≥60% and 50-60%, respectively. The depletion of Pd in gabbroic and basaltic eclogites appears to be associated with the loss of Pd-rich pentlandite probably during high-pressure metamorphism. Rhenium and Pt depletion in the basalts, but not in the gabbros, is likely controlled by degree of hydration, deformation and fluid flow, rather than directly by mineralogy. However, the presence of Pt-rich micro-phases in gabbros provides a possible mechanism by which to retain Pt. The compositional change of sulphide cannot account for Pt and Re depletion due to the very small contribution that sulphide makes to the whole-rock budget of these elements.

Platinum abundances (~350 pg/g) and Pt/Re ratios in gabbros and basalts are not sufficiently high, even if no Pt loss occurs, to generate the radiogenic $^{186}Os/^{188}Os$ ratios or the coupled ^{186}Os-^{187}Os enrichments observed in some mantle-derived melts. However, Pt and Re loss from the down-going slab provides a globally widespread mechanism for the formation of Pt- and Re-rich metasomatised peridotite and/or metasomatic sulphides in the convecting mantle, in a similar way to small degree melt interactions proposed by Luguet et al. (2008b). However, due to the inferred low Pt/Re of slab-derived fluids, a subduction origin for ^{186}Os- and ^{187}Os-enriched mantle material would require either a Pt/Re increase during fluid transport or preferential enrichment of Pt over Re in metasomatic sulphide.

Acknowledgements.

The authors thank the Natural Environment Research Council (NERC) for supporting this work as part of C.D. PhD work, and as part of standard research grant (NE/C51902x/1). We are grateful to Tim Brewer and Sarah Lee for sulphur analyses, Chris Ottley for help with PGE and Re measurements and to Fatima Mokadem for assistance with laser ablation of sulphides. This manuscript was significantly improved following the comments of J.-P. Lorand, I. Puchtel and an anonymous reviewer. We thank M. Rehkamper for his editorial handling and comments.

Word Count:

main text was 13,372, then ~10930 (18% reduction), now 10416(~22% reduction)

abstract: 416

References

Alard, O., Griffin, W.L., Lorand, J.P., Jackson, S.E. and O'Reilly, S.Y., 2000. Non-chondritic distribution of the highly siderophile elements in mantle sulphides. Nature, 407(6806): 891-894.

Amato, J.M., Johnson, C.M., Baumgartner, L.P. and Beard, B.L., 1999. Rapid exhumation of the Zermatt-Saas ophiolite deduced from high-precision Sm-Nd and Rb-Sr geochronology. Earth and Planetary Science Letters, 171(3): 425-438.

Anders, E. and Grevesse, N., 1989. Abundances of the Elements - Meteoritic and Solar. Geochimica Et Cosmochimica Acta, 53(1): 197-214.

Ballhaus, C., Bockrath, C., Wohlgemuth-Ueberwasser, C., Laurenz, V. and Berndt, J., 2006. Fractionation of the noble metals by physical processes. Contributions to Mineralogy and Petrology, 152(6): 667-684.

Barnes, S.J., Naldrett, A.J. and Gorton, M.P., 1985. The Origin of the Fractionation of Platinum-Group Elements in Terrestrial Magmas. Chemical Geology, 53(3-4): 303-323.

Barnicoat, A.C. and Fry, N., 1986. High-Pressure Metamorphism of the Zermatt-Saas Ophiolite Zone, Switzerland. Journal of the Geological Society, 143: 607-618.

Barnicoat, A.C., 1996. V71C-07: Dolomite breakdown under ultra-high pressure conditions in the Allalin Gabbro of SW Switzerland. American Geophysical Union, 77: No. 762.

Barnicoat, A.C. and Cartwright, I., 1997. The gabbro-eclogite transformation: An oxygen isotope and petrographic study of west Alpine ophiolites. Journal of Metamorphic Geology, 15(1): 93-104.

Becker, H., 2000. Re-Os fractionation in eclogites and blueschists and the implications for recycling of oceanic crust into the mantle. Earth and Planetary Science Letters, 177(3-4): 287-300.

Bezos, A., Lorand, J.P., Humler, E. and Gros, M., 2005. Platinum-group element systematics in Mid-Oceanic Ridge basaltic glasses from the Pacific, Atlantic, and Indian Oceans. Geochimica et Cosmochimica Acta, 69(10): 2613-2627.

Birck, J.L., Barman, M.R. and Capmas, F., 1997. Re-Os isotopic measurements at the femtomole level in natural samples. Geostandards Newsletter-the Journal of Geostandards and Geoanalysis, 21(1): 19-27.

Bockrath, C., Ballhaus, C. and Holzheid, A., 2004. Fractionation of the platinum-group elements during mantle melting. Science, 305(5692): 1951-1953.

Borg, L.E., Brandon, A.D., Clynne, M.A. and Walker, R.J., 2000. Re-Os isotopic systematics of primitive lavas from the Lassen region of the Cascade arc, California. Earth and Planetary Science Letters, 177(3-4): 301-317.

Borisov, A., Palme, H. and Spettel, B., 1994. Solubility of Palladium in Silicate Melts - Implications for Core Formation in the Earth. Geochimica Et Cosmochimica Acta, 58(2): 705-716.

Brandon, A.D., Creaser, R.A., Shirey, S.B. and Carlson, R.W., 1996. Osmium recycling in subduction zones. Science, 272(5263): 861-864.

Brandon, A.D., Norman, M.D., Walker, R.J. and Morgan, J.W., 1999. ^{186}Os-^{187}Os systematics of Hawaiian picrites. Earth and Planetary Science Letters, 174(1-2): 25-42.

Brenan, J.M., McDonough, W.F. and Dalpe, C., 2003. Experimental constraints on the partitioning of rhenium and some platinum-group elements between olivine and silicate melt. Earth and Planetary Science Letters, 212(1-2): 135-150.

Brenan, J.M., McDonough, W.F. and Ash, R., 2005. An experimental study of the solubility and partitioning of iridium, osmium and gold between olivine and silicate melt. Earth and Planetary Science Letters, 237(3-4): 855-872.

Capobianco, C.J. and Drake, M.J., 1990. Partitioning of Ruthenium, Rhodium, and Palladium between Spinel and Silicate Melt and Implications for Platinum Group Element Fractionation Trends. Geochimica Et Cosmochimica Acta, 54(3): 869-874.

Capobianco, C.J., Hervig, R.L. and Drake, M.J., 1994. Experiments on Crystal Liquid Partitioning of Ru, Rh and Pd for Magnetite and Hematite Solid-Solutions Crystallized from Silicate Melt. Chemical Geology, 113(1-2): 23-43.

Chesley, J., Ruiz, J., Righter, K., Ferrari, L. and Gomez-Tuena, A., 2002. Source contamination versus assimilation: an example from the Trans-Mexican Volcanic Arc. Earth and Planetary Science Letters, 195(3-4): 211-221.

Chou, C.-L., 1978. Fractionation of siderophile elements in the Earth's upper mantle. Proceedings of the Lunar Planetary Science Conference, IX: 219-230.

Cohen, A.S. and Waters, F.G., 1996. Separation of osmium from geological materials by solvent extraction for analysis by thermal ionisation mass spectrometry. Analytica Chimica Acta, 332(2-3): 269-275.

Creaser, R.A., Papanastassiou, D.A. and Wasserburg, G.J., 1991. Negative Thermal Ion Mass-Spectrometry of Osmium, Rhenium, and Iridium. Geochimica Et Cosmochimica Acta, 55(1): 397-401.

Czamanske, G.K. and Moore, J.G., 1977. Composition and Phase Chemistry of Sulfide Globules in Basalt from Mid-Atlantic Ridge Rift Valley near 37degreesn Lat. Geological Society of America Bulletin, 88(4): 587-599.

Dale, C.W., Gannoun, A., Burton, K.W., Argles, T.W. and Parkinson, I.J., 2007. Rhenium–osmium isotope and elemental behaviour during subduction of oceanic crust and the implications for mantle recycling. Earth and Planetary Science Letters, 253: 211-225.

Dale, C.W., Luguet, A., Macpherson, C.G., Pearson, D.G. and Hickey-Vargas, R., 2008. Extreme platinum-group element fractionation and variable Os isotope compositions in Philippine Sea Plate basalts: Tracing mantle source heterogeneity. Chemical Geology, 248(3-4): 213-238.

Ertel, W., O'Neill, H.S., Sylvester, P.J. and Dingwell, D.B., 1999. Solubilities of Pt and Rh in a haplobasaltic silicate melt at 1300 degrees C. Geochimica Et Cosmochimica Acta, 63(16): 2439-2449.

Ertel, W., O'Neill, H.S., Sylvester, P.J., Dingwell, D.B. and Spettel, B., 2001. The solubility of rhenium in silicate melts: Implications for the geochemical properties of rhenium at high temperatures. Geochimica et Cosmochimica Acta, 65(13): 2161-2170.

Escrig, S., Capmas, F., Dupre, B. and Allegre, C.J., 2004. Osmium isotopic constraints on the nature of the DUPAL anomaly from Indian mid-ocean-ridge basalts. Nature, 431(7004): 59-63.

Escrig, S., Schiano, P., Schilling, J.G. and Allegre, C., 2005. Rhenium-osmium isotope systematics in MORB from the Southern Mid-Atlantic Ridge (40 degrees-50 degrees S). Earth and Planetary Science Letters, 235(3-4): 528-548.

Fleet, M.E., Crocket, J.H. and Stone, W.E., 1996. Partitioning of platinum-group elements (Os, Ir, Ru, Pt, Pd) and gold between sulfide liquid and basalt melt. Geochimica Et Cosmochimica Acta, 60(13): 2397-2412.

Gammons, C.H. and Bloom, M.S., 1993. Experimental Investigation of the Hydrothermal Geochemistry of Platinum and Palladium .2. The Solubility of Pts and Pds in Aqueous Sulfide Solutions to 300-Degrees-C. Geochimica Et Cosmochimica Acta, 57(11): 2451-2467.

Gannoun, A., Burton, K.W., Thomas, L.E., Parkinson, I.J., van Calsteren, P. and Schiano, P., 2004. Osmium isotope heterogeneity in the constituent phases of mid- ocean ridge basalts. Science, 303(5654): 70-72.

Gannoun, A., Burton, K.W., Parkinson, I.J., Alard, O., Schiano, P. and Thomas, L.E., 2007. The scale and origin of the osmium isotope variations in mid-ocean ridge basalts. Earth and Planetary Science Letters, 259(3-4): 541-556.

Harlov, D.E., Newton, R.C., Hansen, E.C. and Janardhan, A.S., 1997. Oxide and sulphide minerals in highly oxidized, Rb-depleted, Archaean granulites of the Shevaroy Hills Massif, South India: Oxidation states and the role of metamorphic fluids. Journal of Metamorphic Geology, 15(6): 701-717.

Holland, T.J.B. and Powell, R., 1985. An Internally Consistent Thermodynamic Dataset with Uncertainties and Correlations .2. Data and Results. Journal of Metamorphic Geology, 3(4): 343-370.

Holland, T.J.B. and Powell, R., 1990. An Enlarged and Updated Internally Consistent Thermodynamic Dataset with Uncertainties and Correlations - the System K2o- Na2o-Cao-Mgo-Mno-Feo-Fe2o3-Al2o3-Tio2-Sio2-C-H2-O2. Journal of Metamorphic Geology, 8(1): 89-124.

Holland, T.J.B. and Powell, R., 1998. An internally consistent thermodynamic data set for phases of petrological interest. Journal of Metamorphic Geology, 16(3): 309-343.

Holzheid, A., Sylvester, P., O'Neill, H.S.C., Rubie, D.C. and Palme, H., 2000. Evidence for a late chondritic veneer in the Earth's mantle from high-pressure partitioning of palladium and platinum. Nature, 406(6794): 396-399.

Keays, R.R., Sewell, D.K.B. and Mitchell, R.H., 1981. Platinum and Palladium Minerals in Upper Mantle-Derived Iherzolites. Nature, 294(5842): 646-648.

Kepezhinskas, P., Defant, M.J. and Widom, E., 2002. Abundance and distribution of PGE and Au in the island-arc mantle: implications for sub-arc metasomatism. Lithos, 60(3-4): 113-128.

Kissin, S.A. and Scott, S.D., 1982. Phase-Relations Involving Pyrrhotite Below 350-Degrees-C. Economic Geology, 77(7): 1739-1754.

Lee, C.T.A., 2002. Platinum-group element geochemistry of peridotite xenoliths from the Sierra Nevada and the Basin and Range, California. Geochimica Et Cosmochimica Acta, 66(22): 3987-4005.

Lorand, J.P., 1985. The Behavior of the Upper Mantle Sulfide Component during the Incipient Alteration of Alpine-Type Peridotites as Illustrated by the Beni-Bousera (Northern Morocco) and Ronda (Southern Spain) Ultramafic Bodies. Tschermaks Mineralogische Und Petrographische Mitteilungen, 34(3-4): 183-209.

Lorand, J.P., Pattou, L. and Gros, M., 1999. Fractionation of platinum-group elements and gold in the upper mantle: a detailed study in Pyrenean orogenic lherzolites. Journal of Petrology, 40(6): 957-981.

Lorand, J.P. and Juteau, T., 2000. The Haymiliyah Sulphide Ores (Haylayn Massif, Oman Ophiolite): In-situ segregation of PGE-poor magmatic sulphides in a fossil oceanic magma chamber. Marine Geophysical Researches, 21(3-4): 327-349.

Lorand, J.P., Luguet, A., Alard, O., Bezos, A. and Meisel, T., 2008. Abundance and distribution of platinum-group elements in orogenic lherzolites; a case study in a Fontete Rouge lherzolite (French Pyrenees). Chemical Geology, 248(3-4): 174-194.

Luguet, A., Alard, O., Lorand, J.P., Pearson, N.J., Ryan, C. and O'Reilly, S.Y., 2001. Laser-ablation microprobe (LAM)-ICPMS unravels the highly siderophile element geochemistry of the oceanic mantle. Earth and Planetary Science Letters, 189(3-4): 285-294.

Luguet, A., Lorand, J.P. and Seyler, M., 2003. Sulfide petrology and highly siderophile element geochemistry of abyssal peridotites: A coupled study of samples from the Kane Fracture Zone (45 degrees W 23 degrees 20N, MARK Area, Atlantic Ocean). Geochimica Et Cosmochimica Acta, 67(8): 1553-1570.

Luguet, A., Lorand, J.-P., Alard, O. and Cottin, J.-Y., 2004. A multi-technique study of platinum group element systematic in some Ligurian ophiolitic peridotites, Italy. Chemical Geology, 208(1-4): 175-194.

Luguet, A., Nowell, G.M. and Pearson, D.G., 2008a. $^{184}Os/^{188}Os$ and $^{186}Os/^{188}Os$ measurements by Negative Thermal Ionisation Mass Spectrometry (N-TIMS): Effects of interfering element and mass fractionation corrections on data accuracy and precision. Chemical Geology, 248(3-4): 342-362.

Luguet, A., Pearson, D.G., Nowell, G.M., Dreher, S.T., Coggon, J.A., Spetsius, Z.V. and Parman, S.W., 2008b. Enriched Pt-Re-Os isotope systematics in plume lavas explained by metasomatic sulfides. Science, 319(5862): 453-456.

Makovicky, E., Makovicky, M. and Rosehansen, J., 1985. Experimental Studies on the Solubility and Distribution of Platinum-Group Elements in Base-Metal Sulfides in Platinum-Group-Mineral Deposits. Canadian Mineralogist, 23: 307-307.

Mathez, E.A., 1976. Sulphur solubility and magmatic sulphides in submarine basalt glass. Journal of Geophysical Research, 81: 4249-4275.

McInnes, B.I.A., McBride, J.S., Evans, N.J., Lambert, D.D. and Andrew, A.S., 1999. Osmium isotope constraints on ore metal recycling in subduction zones. Science, 286(5439): 512-516.

Meisel, T. and Moser, J., 2004. Platinum-group element and rhenium concentrations in low abundance reference materials. Geostandards and Geoanalytical Research, 28(2): 233-250.

Meyer, J., 1983. The development of the high-pressure metamorphism in the Allalin metagabbro (Switzerland). Terra Cognita, 3: 187.

O'Neill, H.S.C. and Mavrogenes, J.A., 2002. The sulfide capacity and the sulfur content at sulfide saturation of silicate melts at 1400 degrees C and 1 bar. Journal of Petrology, 43(6): 1049-1087.

Peach, C.L., Mathez, E.A. and Keays, R.R., 1990. Sulfide Melt Silicate Melt Distribution Coefficients for Noble-Metals and Other Chalcophile Elements as Deduced from MORB - Implications for Partial Melting. Geochimica Et Cosmochimica Acta, 54(12): 3379-3389.

Pearson, D.G., Shirey, S.B., Harris, J.W. and Carlson, R.W., 1998. Sulphide inclusions in diamonds from the Koffiefontein kimberlite, S Africa: constraints on diamond ages and mantle Re-Os systematics. Earth and Planetary Science Letters, 160(3-4): 311-326.

Pearson, D.G. and Woodland, S.J., 2000. Solvent extraction/anion exchange separation and determination of PGEs (Os, Ir, Pt, Pd, Ru) and Re-Os isotopes in geological samples by isotope dilution ICP-MS. Chemical Geology, 165(1-2): 87-107.

Pearson, D.G., Irvine, G.J., Ionov, D.A., Boyd, F.R. and Dreibus, G.E., 2004. Re-Os isotope systematics and platinum group element fractionation during mantle melt extraction: a study of massif and xenolith peridotite suites. Chemical Geology, 208(1-4): 29-59.

Peregoedova, A., Barnes, S.J. and Baker, D.R., 2004. The formation of Pt-Ir alloys and Cu-Pd-rich sulfide melts by partial desulfurization of Fe-Ni-Cu sulfides: results of experiments and implications for natural systems. Chemical Geology, 208(1-4): 247-264.

Peucker-Ehrenbrink, B., Bach, W., Hart, S.R., Blusztajn, J. and Abbruzzese, T., 2003. Rhenium-osmium isotope systematics and platinum group element concentrations in oceanic crust from DSDP/ODP sites 504 and 417/418. Geochemistry Geophysics Geosystems, 4(7): 10.1029/2002GC000414.

Powell, R. and Holland, T.J.B., 1985. An Internally Consistent Thermodynamic Dataset with Uncertainties and Correlations .1. Methods and a Worked Example. Journal of Metamorphic Geology, 3(4): 327-342.

Powell, R. and Holland, T.J.B., 1988. An Internally Consistent Dataset with Uncertainties and Correlations .3. Applications to Geobarometry, Worked Examples and a Computer-Program. Journal of Metamorphic Geology, 6(2): 173-204.

Puchtel, I. and Humayun, M., 2000. Platinum group elements in Kostomuksha komatiites and basalts: Implications for oceanic crust recycling and core-mantle interaction. Geochimica Et Cosmochimica Acta, 64(24): 4227-4242.

Puchtel, I.S., Brandon, A.D., Humayun, M. and Walker, R.J., 2005. Evidence for the early differentiation of the core from Pt-Re-Os isotope systematics of 2.8-Ga komatiites. Earth and Planetary Science Letters, 237(1-2): 118-134.

Rehkämper, M., Halliday, A.N., Fitton, J.G., Lee, D.C., Wieneke, M. and Arndt, N.T., 1999. Ir, Ru, Pt, and Pd in basalts and komatiites: New constraints for the geochemical behavior of the platinum-group elements in the mantle. Geochimica et Cosmochimica Acta, 63(22): 3915-3934.

Reinecke, T., 1991. Very-High-Pressure Metamorphism and Uplift of Coesite-bearing Metasediments from the Zermatt-Saas Zone, Western Alps. European Journal of Mineralogy, 3 (1): 7-17.

Righter, K. and Drake, M.J., 1997. Metal-silicate equilibrium in a homogeneously accreting earth: New results for Re. Earth and Planetary Science Letters, 146(3-4): 541-553.

Roy-Barman, M., Wasserburg, G.J., Papanastassiou, D.A. and Chaussidon, M., 1998. Osmium isotopic compositions and Re-Os concentrations in sulfide globules from basaltic glasses. Earth and Planetary Science Letters, 154(1-4): 331-347.

Rubatto, D., Gebauer, D. and Fanning, M., 1998. Jurassic formation and Eocene subduction of the Zermatt-Saas- Fee ophiolites: implications for the geodynamic evolution of the Central and Western Alps. Contributions to Mineralogy and Petrology, 132(3): 269-287.

Schiano, P., Birck, J.L. and Allegre, C.J., 1997. Osmium-strontium-neodymium-lead isotopic covariations in mid- ocean ridge basalt glasses and the heterogeneity of the upper mantle. Earth and Planetary Science Letters, 150(3-4): 363-379.

Shirey, S.B. and Walker, R.J., 1995. Carius Tube Digestion for Low-Blank Rhenium-Osmium Analysis. Analytical Chemistry, 67(13): 2136-2141.

Sun, W., Bennett, V.C., Eggins, S.M., Arculus, R.J. and Perfit, M.R., 2003. Rhenium systematics in submarine MORB and back-arc basin glasses: laser ablation ICP-MS results. Chemical Geology, 196(1-4): 259-281.

Tatsumi, Y., Oguri, K. and Shimoda, G., 1999. The behaviour of platinum-group elements during magmatic differentiation in Hawaiian tholeiites. Geochemical Journal, 33(4): 237-247.

Van Achtebergh, E., Ryan, C. G., Jackson, S. E. and Griffin, W. L. (2001). Data reduction software for LA-ICP-MS. Laser-Ablation-ICPMS in the Earth Sciences: Principles and Applications, P. J. Sylvester (ed.). Mineral. Assoc. of Canada, Ottawa, Canada: 239-243.

Volkening, J., Walczyk, T. and Heumann, K.G., 1991. Osmium Isotope Ratio Determinations by Negative Thermal Ionization Mass-Spectrometry. International Journal of Mass Spectrometry and Ion Processes, 105(2): 147-159.

Walker, R.J., Prichard, H.M., Ishiwatari, A. and Pimentel, M., 2002. The osmium isotopic composition of convecting upper mantle deduced from ophiolite chromites. Geochimica et Cosmochimica Acta, 66(2): 329-345.

Widom, E., Kepezhinskas, P. and Defant, M., 2003. The nature of metasomatism in the sub-arc mantle wedge: evidence from Re-Os isotopes in Kamchatka peridotite xenoliths. Chemical Geology, 196(1-4): 283-306.

Wood, S.A., Mountain, B.W. and Pan, P., 1992. The Aqueous Geochemistry of Platinum, Palladium and Gold - Recent Experimental Constraints and a Reevaluation of Theoretical Predictions. Canadian Mineralogist, 30: 955-982.

Woodland, S.J., Pearson, D.G. and Thirlwall, M.F., 2002. A platinum group element and Re-Os isotope investigation of siderophile element recycling in subduction zones: Comparison of Grenada, Lesser Antilles arc, and the Izu-Bonin arc. Journal of Petrology, 43(1): 171-198.

FIGURE CAPTIONS

Figure 1. Composite sulphide grains from (a) gabbro S02/83vix and (b) gabbroic eclogite S01/40iiix. (a) Sulphide located between olivine and plagioclase. Pyrrhotite (Po) is the major gabbroic sulphide phase, but significant amounts of pentlandite (Pn) are also present. Chalcopyrite (Cp) is a minor constituent and usually forms at sulphide-silicate boundaries. The relative proportions of the three phases vary between grains, and also between samples. (b) Eclogitic sulphides have been recrystallised, are considerably larger and consist mainly of pyrite (Py), probably due to the addition of a sulphur-rich, iron-poor fluid, either during seafloor alteration or HP metamorphism. The grain pictured is unusual in the limited extent to which Py has formed. Note the absence of Pn and the retention of some Cp, although many eclogitic sulphides consist entirely of pyrite.

Figure 2. Chondrite-normalised PGE-Re patterns for (a) gabbros, (b) gabbroic eclogites. Gabbros typically have smooth, fractionated PGE patterns with PPGE>IPGE, but less inter-element fractionation than the current MORB mean. Transitional gabbros are shown as light grey dashed lines in (a) and the corresponding gabbro is a black line with the same ornament. There is little variation (and no systematic variation) between transitional and preserved gabbros. Gabbroic eclogites display much greater variability and Pd concentrations are much lower than in the gabbros. CI chondrite values from Anders and Grevesse (1989).

Figure 3. Relative mean difference in PGE and Re concentrations between gabbroic eclogite and precursor gabbro (darker shade, circles) and between basaltic eclogite and MORB (lighter shade, diamonds). Each mean is based on a small sample number (n=8) with a large range of PGE concentrations and so the standard deviation (SD) of each mean is approximately equal to the mean itself. Values used for MORB are, in pg/g: Os - 9, Ir* - 10, Ru - 47, Pt - 343, Pd - 666 and Re - 1100 (Schiano et al. 1997; Rehkämper et al. 1999; Escrig et al. 2004, Bezos et

al. 2005; Escrig et al. 2005, Gannoun et al. 2007). * The current MORB mean for Ir is around 30 pg/g but given the mean for Os of <10pg/g from a greater number of samples, and their similar behaviour, a value of 10 pg/g Ir has been used.

Figure 4. Chondrite-normalised PGE/Ir variations with MgO for gabbros (dark field), gabbroic eclogites (G. eclogite, mid-shade field) and basaltic eclogites (B). Best-fit lines drawn by eye through the gabbro data. Os data are 'common Os' –calculated by subtraction of ingrown ^{187}Os. MORB data (light fields) from [1] Bezos et al. (2005) and [2] Rehkamper et al. (1999), CI chondrite values from Anders and Grevesse (1989).

Figure 5. PGE-Re patterns for ZSO basaltic eclogites. Thick dashed line is basaltic eclogite mean excluding high Pt sample. Basaltic eclogites contain significantly less Re, Pt and Pd than the MORB average estimate (details of which in Figure 3 caption). CI chondrite values: Anders and Grevesse (1989).

Figure 6. Chondrite-normalised PGE-Re patterns for laser-ablated sulphides from gabbros (a-b) and gabbroic eclogites (c-d). Symbol shapes denote host sample, colours denote sulphide type: Po – pyrrhotite, Pn – pentlandite, Cp – chalcopyrite, Py –pyrite. Legend ornaments are end-members, some analyses shown are composites indicated by combinations of colour. Small points indicate a large uncertainty due to interference or detection limit, and usually represent an upper limit. Dashed lines link such data+ to other data. (a) Igneous pyrrhotites are characterised by a small degree of fractionation except for Pt, which has low normalised concentrations; (b) & (d) Chalcopyrite and pentlandite have higher Pd/Ir and Re/Os ratios; (c) Pyrites in gabbroic eclogites display greater fractionation of the PGE, with much higher Re/Os ratios than igneous sulphides, and appear to define two groups, which we have termed I and II. CI chondrite values: Anders and Grevesse (1989).

Figure 7. Pd vs. Os, Re and Pt for gabbro- and gabbroic eclogite-hosted sulphides (G and GE, respectively). Symbol colour and shape define sulphides from a single sample, ornament denotes sulphide type (commonly a composite analysis). Where present, dashed arrows indicate the plotted concentration is the detection limit, and the arrow indicates the direction of the 'true' concentration.

Figure 8. Pd vs Ni and Pt vs Ni for sulphides from gabbros (G, squares) and gabbroic eclogites (GE, circles). Pd clearly co-varies positively with nickel in gabbroic sulphides (r^2 = 0.98 for sample 83vix). There is little or no co-variation for eclogitic sulphides, which have lower Ni and Pd abundances and a smaller range of Ni content. Neither gabbroic nor eclogitic sulphides display co-variation between Ni and Pt. Small symbols signify Pd detection limit for analysis and are therefore only an upper constraint.

Figure 9. Os vs. Re for individual silicate, oxide and sulphide mineral phases from two gabbros and two gabbroic eclogites. Sulphide data for S01/39iiix includes in situ data from S01/36ix which has comparable whole-rock PGE concentrations.

Figure 10. Re-Os model age plotted against elemental Re/Os ratio for whole-rock and mineral analyses from two gabbros (S01/39iiix, black symbols; S02/83vix, blue) and one gabbroic eclogite (S01/3iix, light/unfilled symbols). Igneous mineral phases are typically close to, or within uncertainty of, the age of igneous crystallisation. Eclogitic mineral model ages have been calculated using the isotopic composition of the whole-rock at 45Ma (the timing of HP metamorphism, $^{187}Os/^{188}Os$ = 0.17). Eclogitic phases have model ages which are consistent with mineral-scale resetting of the Re-Os system during HP metamorphism. Note the difference in Re/Os ratios observed in gabbroic and eclogitic sulphides.

Figure 11. Estimated contributions of constituent phases to the whole-rock Os and Re budget for a gabbro (S01/39iiix) and a gabbroic eclogite (S01/3iix), scaled to 100%. Due to limited sulphide Re data for S01/39iiix, in situ data from S01/36ix, which has a similar whole-rock Re concentration, has been incorporated.

Figure 12. Approximate average percentage of whole-rock PGE and Re hosted by sulphides in (a) gabbros (n=3) and (b) gabbroic eclogites (n=4). Given that sulphides in one particularly PGE-rich gabbro, S02/6ix, only account for <30% of the IPGE and <10% of the Pd, the typical proportion of IPGE and Pd hosted in gabbroic sulphides is likely to be closer to 100%.

Figure 13. Schematic cross section of a subduction zone illustrating probable elemental fluxes, and possible generation of Pt- and Re-enriched mantle that could form a source of coupled enrichments of ^{186}Os and ^{187}Os.

TABLES

Table 1. Major element compositions of typical sulphides from a gabbro and a gabbroic eclogite, determined by electron probe micro-analysis.

	Gabbro			Gabbroic eclogite		
	Po	**Pn**	**Cp**	**Py**	**Po**	**Cp**
S	38.38	32.48	34.81	53.18	39.27	34.99
Fe	61.30	40.51	30.82	46.55	59.47	30.71
Co	0.05	1.62	0.01	0.66	0.39	0.02
Ni	0.41	25.69	0.02	0.00	0.38	0.01
Zn	0.00	0.00	0.00	0.00	0.00	0.00
Cu	0.03	0.07	32.70	0.00	0.49	32.55
Cr	0.01	0.02	0.00	0.00	0.00	0.00
Tot	100.2	100.3	98.37	100.3	100.0	98.27
M/S	0.92	1.18	0.98	0.51	0.89	0.97

Notes: Po – pyrrhotite, Pn – pentlandite, Cp – chalcopyrite, Py – pyrite.

Composition and atomic metal/sulphur (M/S) ratios of pyrrhotites indicate a change in structure between gabbros and gabbroic eclogites, from hexagonal towards monoclinic (cf. Lorand and Juteau, 2000). In some cases, pyrrhotite in gabbros has been altered to troilite.

Table 2. PGE and Re concentrations and Re-Os isotopes in ZSO gabbros, gabbroic eclogites, transitional gabbros and basaltic eclogites

	Mass (g)	Os* ng/g	**Os** ng/g	**Ir** ng/g	**Ru** ng/g	**Pt** ng/g	**Pd** ng/g	**Re** ng/g	**$^{187}Os/^{188}Os^{\alpha}$**	**$^{187}Re/^{188}Os$**	**Model Age$^{\lambda}$**	**MgO** wt.%	**Ni** µg/g	**S** µg/g	**Yb** µg/g
Gabbros															
S01/5G	1.999	0.0104	0.0108	0.0074	0.021	0.131	0.096	0.202	0.3795 ± 0.0003	92.7	157	14.1	385	328	0.14
S01/36ix	1.000	0.0185	0.0189	0.013	0.031	0.232	0.122	0.189	0.2827 ± 0.0004	49.2	179	9.17	313	438	0.20
dupl [§§]	1.015	0.0196	0.0200	0.014	0.031	0.256	0.135	0.195	0.2770 ± 0.0005	47.9	177	-	-	-	-
S01/39iiix	1.065	0.0095	0.0097	0.0055	0.011	0.092	0.049	0.144	0.3114 ± 0.0002	73.5	143	10.3	386	311	0.18
S02/6ix	0.970	0.320	0.321	0.322	0.581	1.20	1.78	0.406	0.1502 ± 0.0001	6.11	149	17.7	546	1073	0.62
S02/10iiixG	1.016	0.063	0.063	0.047	0.081	0.590	1.37	0.102	0.1753 ± 0.0001	7.89	307	6.65	184	286	0.08
dupl.[§]	1.075	0.065	0.066	0.045	0.077	0.611	1.36	0.098	0.1756 ± 0.0001	7.25	339	-	-	-	-
dupl [§§]	1.018	-	-	0.045	0.069	0.519	1.45	0.087	0.1753 ± 0.0001	-	-	-	-	-	-
S02/83vix	1.031	0.075	0.075	0.056	0.125	0.559	0.716	0.290	0.1934 ± 0.0002	18.7	184	13.4	363	696	0.38
S02/83viix	1.503	0.0020	0.0023	0.0016	<0.010	0.019	0.013	0.179	1.180 ± 0.002	434	145	8.88	154	463	0.80
S02/83viiixG	1.006	0.0069	0.0071	0.0046	0.011	0.083	0.083	0.136	0.4109 ± 0.0005	94.5	174	10.7	349	355	0.19
		Mean	*0.064*	*0.057*	*0.108*	*0.363*	*0.532*	*0.206*							
		Mean[#]	*0.027*	*0.019*	*0.041*	*0.243*	*0.355*	*0.177*							
		Median	*0.015*	*0.011*	*0.026*	*0.187*	*0.112*	*0.185*							
Transitional															
S01/5E	1.057	0.0172	0.0178	0.011	0.025	0.134	0.068	0.401	0.4051 ± 0.0003	112	144	11.8	420	961	0.21
S02/10iiixE	1.159	0.038	0.039	0.026	0.050	0.566	0.979	0.203	0.2236 ± 0.0001	25.6	206	9.27	263	211	0.15
S02/83viiixE	1.025	0.0087	0.0089	0.0060	0.020	0.113	0.057	0.316	0.3634 ± 0.0003	176	77	11.1	369	407	0.18
		Mean	*0.022*	*0.014*	*0.031*	*0.271*	*0.368*	*0.307*							
Gabbroic eclogites															
S01/3iix	2.000	0.104	0.105	-	0.076	*12.8*	0.176	0.475	0.1767 ± 0.0001	22.1	133	7.80	172	549	0.37
dupl.[§]	1.022	0.098	0.098	0.073	0.083	0.937	0.073	0.131	0.1776 ± 0.0001	6.48	401	-	-	-	-
dupl [§]	1.082	0.099	0.099	0.079	0.075	0.835	0.082	0.124	0.1769 ± 0.0001	6.04	424	-	-	-	-
dupl [§§]	1.016	-	-	0.072	0.074	0.786	0.079	0.102	-	-	-	-	-	-	-
S01/35iix	1.035	0.045	0.045	0.039	0.089	0.095	0.103	0.221	0.2101 ± 0.0001	23.8	187	8.35	204	466	0.37
S01/35iiix	1.098	0.055	0.056	0.045	0.095	0.160	0.071	0.546	0.2431 ± 0.0001	47.6	135	7.03	124	920	0.78
S01/40iiix	1.010	0.0090	0.0092	0.0048	0.016	0.124	0.046	0.117	0.2755 ± 0.0001	62.7	133	12.3	385	167	0.13
S01/40vx	1.056	0.0192	0.0194	0.015	0.023	0.332	0.168	0.081	0.2001 ± 0.0001	20.4	189	11.9	292	146	0.23
S01/40viix	1.053	0.0115	0.0117	0.0071	-	0.124	0.123	0.068	0.2266 ± 0.0002	28.3	193	12.3	348	152	0.23
dupl.[§]	1.091	0.0128	0.0130	0.0069	0.018	0.150	0.111	0.067	0.2279 ± 0.0002	25.3	219	-	-	-	-
S02/84viix	1.759	0.0009	0.0016	0.0010	<0.006	0.013	0.019	0.387	6.081 ± 0.007	2076	172	8.84	156	555	1.23
S02/85ixE	0.908	0.0033	0.0035	0.0029	0.0069	0.199	0.0094	0.150	0.7523 ± 0.0008	222	167	6.80	149	255	0.66
		Mean	*0.031*	*0.024*	*0.041*	*0.243*	*0.080*	*0.227*							
		Median	*0.016*	*0.011*	*0.020*	*0.149*	*0.087*	*0.179*							
		Total gabbroic mean	*0.043*	*0.036*	*0.068*	*0.298*	*0.316*	*0.230*							
		Total gabbroic median	*0.018*	*0.011*	*0.023*	*0.137*	*0.096*	*0.202*							

	Mass (g)	Os* ng/g	**Os** ng/g	**Ir** ng/g	**Ru** ng/g	**Pt** ng/g	**Pd** ng/g	**Re** ng/g	**$^{187}Os/^{188}Os^{\alpha}$**	**$^{187}Re/^{188}Os$**	**Model Age$^{\lambda}$**	**MgO** wt.%	**Ni** µg/g	**S** µg/g	**Yb** µg/g
Basaltic eclogites															
S02/41ii	1.034	0.0039	0.0111	0.0034	0.016	0.027	0.065	0.606	14.30 ± 0.01	753	1120	5.20	46	1907	5.27
S02/41v	1.016	0.0027	0.0029	0.0011	0.016	0.041	0.091	0.120	0.7790 ± 0.0008	216	179	5.51	56	1210	4.87
dupl §§	1.034	-	-	0.0016	0.012	0.051	0.085	0.100	-	-	-	-	-	-	-
S02/74ii	1.092	0.0120	0.0132	0.0099	0.035	0.059	0.063	0.827	0.8634 ± 0.0006	332	131	6.17	113	1287	3.43
S02/75iiR	1.098	0.0120	0.0122	0.0078	0.021	0.437	0.050	0.062	0.2904 ± 0.0002	24.8	377	5.31	73	712	4.31
S02/75iiiC	1.012	0.0088	0.0096	0.011	0.034	0.057	0.029	0.237	0.8344 ± 0.0005	130	323	5.63	72	932	4.92
S02/75iiiR	1.022	0.0095	0.0103	0.0096	0.034	0.048	0.038	0.540	0.7441 ± 0.0005	274	133	6.46	91	538	3.82
	Mean	*0.008*	*0.010*	*0.007*	*0.026*	*0.112*	*0.055*	*0.397*							
	Median	*0.009*	*0.011*	*0.009*	*0.028*	*0.052*	*0.056*	*0.389*							
Reference materials															
DR26 type 1	*1.003*		*0.014*	*0.007*	*-*	*0.359*	*1.26*	*0.443*	*0.2386 ± 0.0002*	*149*	*44*				
dupl §§	*1.005*		*0.020*	*0.015*	*0.081*	*0.673*	*1.49*	*0.534*	*0.2640 ± 0.0002*	*128*	*64*				
dupl §§	*1.006*		*0.015*	*0.012*	*0.073*	*0.421*	*1.44*	*0.506*	*0.2228 ± 0.0002*	*160*	*35*				
Paris mean			*-*	*0.054±0.095*	*0.064±0.022*	*0.64±0.37*	*1.38±0.15*	*-*							
EN026 10D-3	*1.005*		*0.010*	*0.012*	*0.031*	*0.286*	*0.670*	*0.483*	*0.1697 ± 0.0029*	*233*	*11*				
dupl §	*1.997*		*0.008*	*0.011*	*0.030*	*0.218*	*0.690*	*0.470*	*0.1585 ± 0.0018*	*284*	*6.3*				
MUL mean			*0.018±0.054*	*0.036±0.034*	*0.041±0.007*	*0.37±0.12*	*0.72±0.09*	*0.516±0.057*	*0.137 ± 0.008*						
WHOI mean			*0.017±0.013*	*0.027±0.014*	*-*	*0.60±0.46*	*1.47±0.25*	*-*	*0.160±0.013*						
URI mean			*-*	*0.019±0.012*	*0.047±0.010*	*0.84±0.14*	*1.75±0.39*	*1.38±0.52*							
TDB-1	1.010		0.104	0.059	0.191	4.63	24.7	0.809	0.9688 ± 0.0003	41.5	1214				
dupl §§	1.011		-	0.061	0.256	5.82	34	0.978	0.9077 ± 0.0003	-	-				
MUL mean			*0.117±0.028*	*0.075±0.023*	*0.198±0.020*	*5.01±0.45*	*24.3±4.6*	*0.794±0.057*	*0.92 ± 0.20*	*35.9±10.1*	*1322±90*				
WHOI mean			*0.122±0.016*	*0.078±0.014*	*-*	*4.40±0.66*	*24.8±2.5*	*-*	*-*						

Notes:

Comprehensive major and trace element data available in the supplementary online material of Dale et al. (2007).

Significant figures: In order to permit accurate use of the data (e.g. low concentration Os/Ir ratios, which are readily reproducible) concentrations of some samples are quoted to 4 significant figures; such precision is reasonable for individual dissolutions. However, duplicate digestions demonstrate that the overall uncertainty for sample concentration, discussed in the text, is considerably greater.

Os* is the Os concentration after subtraction of ingrown ^{187}Os

Mean#: This is the average gabbro composition, omitting sample S02/6ix, which has anomalously high PGE concentrations. Omission, which gives similar means for gabbros and gabbroic eclogites, is justified by Os isotope data that demonstrate no significant change of Os concentrations by metamorphism.

$^{\alpha}$ Isotope ratios are blank corrected. Uncertainties are 2σ mean; $^{187}Os/^{188}Os$ ratios normalised using $^{192}Os/^{188}Os$=3.08271 & corrected using $^{18}O/^{16}O$ and $^{17}O/^{16}O$ of 0.002045 and 0.000371 respectively.

$^{\lambda}$ Model ages were calculated using $TMa=1/\lambda*Ln[(^{187}Os/^{188}Os_{isochron}-^{187}Os/^{188}Os_{sample})/(^{187}Re/^{188}Os_{chond}-^{187}Re/^{188}Os_{sample})+1]/1000000$, where $^{187}Os/^{188}Os_{isochron}$ is the initial (0.137) of the errochron defined by these samples in Dale et al. (2007).

The Pt concentration in grey italics is thought to be due to the so-called 'nugget effect', which can affect small sample mass digestions, and is probably unrepresentative.

§ Replicate analyses of the same powder, through repeated chemistry.

§§ Replicate analyses of the same powder, through repeated chemistry, including an initial HF-HCl desilicification step.

Reference material data in italics previously published in Dale et al., (2008). Published means and uncertainties for reference materials (also in italics, Paris – IPGP / MNHN, Bezos et al. (2005); MUL – Mulhouse and URI – University of Rhode Island, Meisel and Moser (2004) and ref. therein; WHOI – Woods Hole Oceanographic Institution, Peucker-Ehrenbrink et al. (2003).

Table 3. HSE concentrations (µg/g) and estimated contribution of each sulphide end-member for laser-ablation ICP-MS analyses of gabbro- and gabbroic eclogite hosted sulphides. Po – pyrrhotite, Pn – pentlandite, Cp – chalcopyrite, Py – pyrite. Ru and Rh data in grey italics carry greater uncertainties due to argide interferences. For other data, where '<' is used, the value quoted is defined by the detection limit.

	S01/36ix (G)							***S02/6ix (G)***						
	Po	**Po**	**Po**	**Po(Pn)**	**Pn/Po**	**Po/Cp(Pn)**	**Cp/Po/Py**	**Po**	**Po**	**Po**	**Po**	**Po/Pn(Cp)**	**Pn(Po)**	**Pn/Cp(Po)**
% Po	100	97	94	89	51	54	37	100	99	99	98	72	21	20
% Pn	-	3	3	10	49	12	21	-	1	-	1	13	76	57
% Cp	-	1	3	1	0	35	41	-	1	1	-	15	3	23
Os	0.050	0.047	0.045	0.034	0.027	0.032	0.017	0.018	0.018	<0.011	0.059	0.053	<0.013	0.048
Ir	0.034	0.039	0.018	0.019	0.014	0.017	<0.003	0.009	0.006	0.019	0.014	0.024	0.023	0.018
Ru *	*<0.142*	*<0.081*	*<0.243*	0.049	*<0.090*	0.067	0.033	0.016	0.023	<0.051	0.073	*<0.125*	*<0.411*	*<0.160*
Rh **	0.001	*<0.032*	-	*<0.06*	<0.003	*0.072*	*0.129*	<0.001	*0.006*	0.036	0.014	-	-	-
Pt	0.006	0.003	<0.002	<0.003	<0.004	<0.003	0.009	<0.002	<0.002	<0.016	<0.009	<0.007	<0.017	0.090
Pd	0.015	0.026	<0.005	0.072	0.192	0.092	0.169	0.017	0.021	0.090	0.035	0.364	0.226	<0.083
Re	0.006	0.011	0.002	0.006	0.009	0.076	0.003	0.003	0.002	<0.008	<0.004	0.010	0.015	0.042
Au	<0.002	<0.002	<0.002	<0.002	<0.003	<0.002	0.004	<0.002	<0.002	<0.010	<0.006	0.025	<0.012	<0.022
Ag	0.232	0.377	0.446	0.571	0.121	2.85	2.05	0.106	0.048	0.404	0.372	0.83	0.561	1.20

	S02/83vix (G)												***S02/84viix (GE)***		
	Po	**Po**	**Po(Cp)**	**Po(Pn)**	**Po(PnC**	**Po/Pn**	**Pn/Po**	**Pn**	**Pn(Cp)**	**Cp/Pn**	**Cp**	**Po/Cp**	**Py**	**Py**	**Py**
% Py	-	-	-	-	-	-	-	-	-	-	-	-	98	100	100
% Po	99	95	91	88	85	55	39		-			70	-	-	-
% Pn	1	2	1	12	8	39	58	105	90	45	4	8	-	-	-
% Cp	-	3	8	1	7	6	3	2	10	57	105	22	2	-	-
Os	0.028	0.011	0.028	0.067	0.126	<0.004	<0.003	0.023	<0.004	<0.005	<0.021	0.321	0.002	0.003	0.002
Ir	0.014	0.010	0.015	0.015	0.080	0.004	<0.002	0.016	0.004	0.005	<0.013	0.140	0.002	0.002	0.001
Ru *	0.034	0.042	0.033	*<0.050*	*<0.204*	*<0.178*	*<0.301*	*<0.495*	*<0.524*	*<0.275*	0.171	*<0.220*	<0.005	<0.012	<0.008
Rh **	0.002	*0.028*	*0.012*	0.027	*0.050*	-	*<0.21*	*0.027*	*0.008*	-	-	-	-	0.007	0.004
Pt	0.003	0.004	0.007	0.022	0.017	<0.005	0.006	<0.002	0.010	0.017	0.058	0.057	0.006	0.023	0.008
Pd	0.030	0.067	0.049	0.253	0.150	0.886	1.266	1.982	1.453	0.783	0.102	0.224	0.032	<0.009	<0.007
Re	0.003	0.006	0.010	0.011	0.010	0.090	0.003	0.003	0.004	0.011	<0.013	0.022	0.131	0.073	0.127
Au	<0.002	0.009	<0.002	0.002	0.014	0.011	<0.003	0.003	<0.003	0.005	<0.019	0.003	0.038	<0.003	<0.002
Ag	0.915	2.39	1.14	5.63	3.40	3.90	4.33	2.97	16.3	9.65	3.05	5.91	1.24	0.779	0.077

	S01/3iix (GE)						***S01/40iiix (GE)***					***S02/85ixE (GE)***			
	Py	**Py**	**Py**	**Py**	**Py**	**Po/Cp**	**Py**	**Py**	**Po**	**Po/Cp**	**Cp/Py**	**Py**	**Py**	**Py**	**Po(Cp)**
% Py	100	99	100	96	100		99	99		67	45	99	100	100	-
% Po	-	-	-	-	-	78	-	-	98	-	-	-	-	-	87
% Pn	-	-	-	-	-	1	1	1	2	5	1	1	-	-	1
% Cp	-	1	-	3	-	22	-	-	-	27	54	-	-	-	12
Os	0.004	0.015	0.072	0.112	0.204	0.007	0.002	0.001	0.001	0.002	0.005	0.001	0.003	0.001	0.004
Ir	0.001	0.004	0.046	0.137	0.192	0.003	0.001	0.001	0.001	0.001	0.002	0.001	0.003	0.001	0.002
Ru *	0.003	0.004	0.021	0.042	0.070	0.022	0.008	<0.006	0.012	*<0.031*	0.045	<0.003	0.004	<0.005	<0.010
Rh **	0.001	*<0.058*	<0.014	*0.015*	0.022	-	0.002	<0.009	*<0.019*	-	-	<0.001	0.002	<0.001	-
Pt	0.043	0.062	0.170	0.167	0.125	0.025	0.004	0.009	0.002	0.026	0.081	<0.001	<0.001	0.002	<0.003
Pd	0.009	0.015	0.007	0.013	0.012	0.322	0.012	<0.004	0.014	0.054	0.098	<0.002	0.005	0.005	0.039
Re	0.041	0.005	0.021	0.009	0.009	0.004	0.007	0.011	0.031	0.022	0.052	0.002	0.002	0.019	0.033
Au	0.001	0.020	0.001	<0.003	<0.004	0.039	<0.001	<0.002	<0.001	<0.002	0.003	0.001	0.001	<0.001	0.044
Ag	0.062	0.217	0.680	3.62	0.028	2.21	0.033	0.071	0.140	2.31	2.83	0.024	0.031	0.121	3.83

Table 4. Re-Os abundances and isotope data for separated silicate and sulphide phases from two gabbros and two eclogites. Data obtained by isotope-dilution N-TIMS.

	Mass (mg)	Re (ng/g)	Os (ng/g)	Os* (ng/g)	$^{187}Os/^{188}Os$	$^{187}Re/^{188}Os$	Blank (%)[‡] Os	Blank (%)[‡] Re	Model age[a]	Model age[b]	Prop. W.R.(%)[#] Os	Prop. W.R.(%)[#] Re
Gabbros												
S01/39iiix												
Whole rock	*460.1*	*0.139*	*0.011*	*0.011*	*0.3336 ± 0.0042*	*61.3 ± 3*	*7*	*19*	*194*	-	-	-
dupl.	*406.6*	*0.204*	*0.020*	*0.020*	*0.3005 ± 0.0028*	*50.4 ± 1*	*1*	*5.4*	*196*	-	-	-
dupl.[§]	1061	0.144	0.010	0.009	0.3114 ± 0.0002	74 ± 2	1	1	143	-	-	-
Silicates												
Olivine	380.8	0.024	0.0067	0.0066	0.217 ± 0.007	17.3 ± 0.5	2	12	285	-	9	3
Olivine	2.00	0.71	0.045	0.044	0.275 ± 0.021	79 ± 21	12	60	105	-	59	164
Olivine	45.39	0.35	0.024	0.024	-	71 ± 9	5	7	-	-	31	42
Plagioclase	64.75	0.17	<0.0005	-	-	~4000	80	10	-	-	1	67
Augite	44.26	0.12	0.001	0.001	1.414 ± 0.174	510 ± 100	47	19	150	-	1	8
Oxides												
Opaques (Ilmenite & Al-chromite)	1.83	1.13	0.128	0.127	0.167 ± 0.006	43 ± 9	5	55	45	-	4	5
Sulphides	(µg)											
Sulphide[m]	27.30	-	9.3	8.7	0.678 ± 0.012	-	4		-	-	50	*341*
Sulphide[m]	9.00	-	19.1	18.5	0.340 ± 0.010	-	6	-	-	-	103	-
Sulphide	15460	37.4	36.7	36.6	0.144 ± 0.000	4.9 ± 0.1	0	0.2	119	-	198	*18*
S01/83vix												
Whole rock	*411.0*	*0.288*	*0.081*	*0.081*	*0.1926 ± 0.0008*	*17.2 ± 0.2*	*1*	*11.6*	*199*	-	-	-
dupl.	*2093*	*0.313*	*0.079*	*0.078*	*0.1941 ± 0.0001*	*19.3 ± 0.3*	*0*	*1.4*	*181*	-	-	-
dupl.	*305.4*	*0.276*	*0.079*	*0.078*	*0.1935 ± 0.0006*	*16.9 ± 0.3*	*0*	*11*	*205*	-	-	-
dupl.[§]	1031	0.290	0.075	0.075	0.1934 ± 0.0002	18.7 ± 0.2	0	11	184	-	-	-
Silicates												
Olivine	10.36	0.42	0.019	0.019	0.184 ± 0.006	109 ± 11	6	33	26	-	-	-
Augite	24.34	0.048	0.003	0.003	0.411 ± 0.041	85 ± 38	16	65	195	-	-	-
Olivine (many opaque inclusions)	1.52	0.78	0.36	0.36	0.161 ± 0.015	12 ± 3	2	48	134	-	-	-
Gabbroic eclogites												
S01/3iix												
Whole rock	*419.9*	*0.220*	*0.048*	*0.047*	*0.1944 ± 0.0013*	*22.4 ± 0.3*	*0*	*4*	*157*	-	-	-
dupl.	*398.2*	*0.233*	*0.057*	*0.057*	*0.1890 ± 0.0005*	*19.8 ± 2.1*	*1*	*35*	*161*	-	-	-
dupl.[§]	2000	0.475	0.105	0.104	0.1767 ± 0.0001	22.1 ± 0.2	0	0	110	-	-	-
dupl.[§]	1022	0.131	0.098	0.098	0.1776 ± 0.0001	6.5 ± 0.3	1	1	401	-	-	-
dupl.[§]	1082	0.124	0.099	0.099	0.1769 ± 0.0001	6.0 ± 0.2	0	0	424	-	-	-
dupl.[§§]	1016	0.102	-	-	-	-	-	2	-	-	-	-
Silicates												
Garnet	24.53	7.2	0.048	0.048	0.168 ± 0.002	722 ± 21	1	1	3	0	3	147
Saussurite	21.75	0.075	0.005	0.005	0.210 ± 0.011	68 ± 20	10	9	65	35	4	26
Saussurite	95.04	0.14	0.010	0.010	0.446 ± 0.003	66 ± 2	5	52	282	252	7	33
Omphacite	16.38	0.30	0.033	0.033	0.214 ± 0.003	45 ± 3	2	20	104	59	1	2
Glaucophane	88.12	0.13	0.091	0.091	0.175 ± 0.001	6.8 ± 0.2	1	10	355	44	15	9
Talc	6.36	0.35	0.15	0.15	0.177 ± 0.004	11 ± 2	1	49	223	38	11	13
Sulphides	(µg)											
Sulphide	1793	14.7	31.5	31.3	0.184 ± 0.001	2.3 ± 0.1	1	4	1525	465	47	8
Sulphide	2750	28.2	0.49	0.48	0.367 ± 0.010	285 ± 17	21	1	48	42	0.7	15
Sulphide	1135	101	2.23	2.21	0.181 ± 0.001	220 ± 7	13	1	12	3	3	52
Sulphide	620.0	53.7	0.41	0.41	0.718 ± 0.021	672 ± 20	5	4	52	49	0.7	28
Sulphide	200.0	71.6	0.37	0.36	1.21 ± 0.14	1056 ± 132	15	9	61	59	0.6	38
Sulphide[m]	69.80	-	15.3	15.1	0.204 ± 0.003	-	1	-	-	-	23	-
Sulphide[m]	59.60	-	1.30	1.26	0.380 ± 0.033	-	11	-	-	-	2	-
S01/39ix												
Whole rock	2118	-	0.0053	0.0052	0.2187 ± 0.0140	-	4	-	-	-	-	-
Silicates												
Garnet	24.53	1.01	0.008	0.008	0.157 ± 0.003	580 ± 17	3	3	2	0	-	-
Cr-omphacite	35.32	-	0.013	0.013	0.148 ± 0.003	6.6 ± 3.0	3	-	-	-	-	-
Talc	16.52	0.60	0.020	0.019	0.197 ± 0.005	149 ± 24	4	18	25	15	-	-
Chloritoid	14.62	0.15	0.004	0.004	0.491 ± 0.034	163 ± 34	16	37	105	98	-	-
Sulphides	(µg)											
Sulphide	930.0	95.9	0.41	0.374	0.974 ± 0.010	1236 ± 37	3	1	41	40	-	-

Notes: See notes in Table 2 for Os* and uncertainties.
Blank (%)[‡] - the % contribution of the total procedural blank to the total Os or Re measured
Model age[a] – see Table 2; Model age[b] - calculated using an initial $^{187}Os/^{188}Os$ of 0.17, corresponding to the whole rock ratio at 45 Ma.
Prop. W.R.(%)[#] - the proportion of the whole rock budget of Os and Re which would be hosted by each phase, based on each individual measurement of the Os and Re concentration, hence the total is >>100%. An estimation of the 'true' average contribution of each phase has been made and is presented in Figure 11, and is discussed in the text.
Data in italics – previously published in Dale et al., (2007).
dupl. - Replicate analysis of the same powder, through repeated HF-HBr dissolution chemistry.
dupl.[§] - Replicate analysis of the same powder, through repeated high-pressure asher (HPA) digestion and chemistry.
dupl.[§§] - Replicate analysis of the same powder, through repeated HPA digestion and chemistry, including an initial HF-HCl desilicification step.
Sulphide[m] – Digestion and purification by microdistillation only.

Figure 1

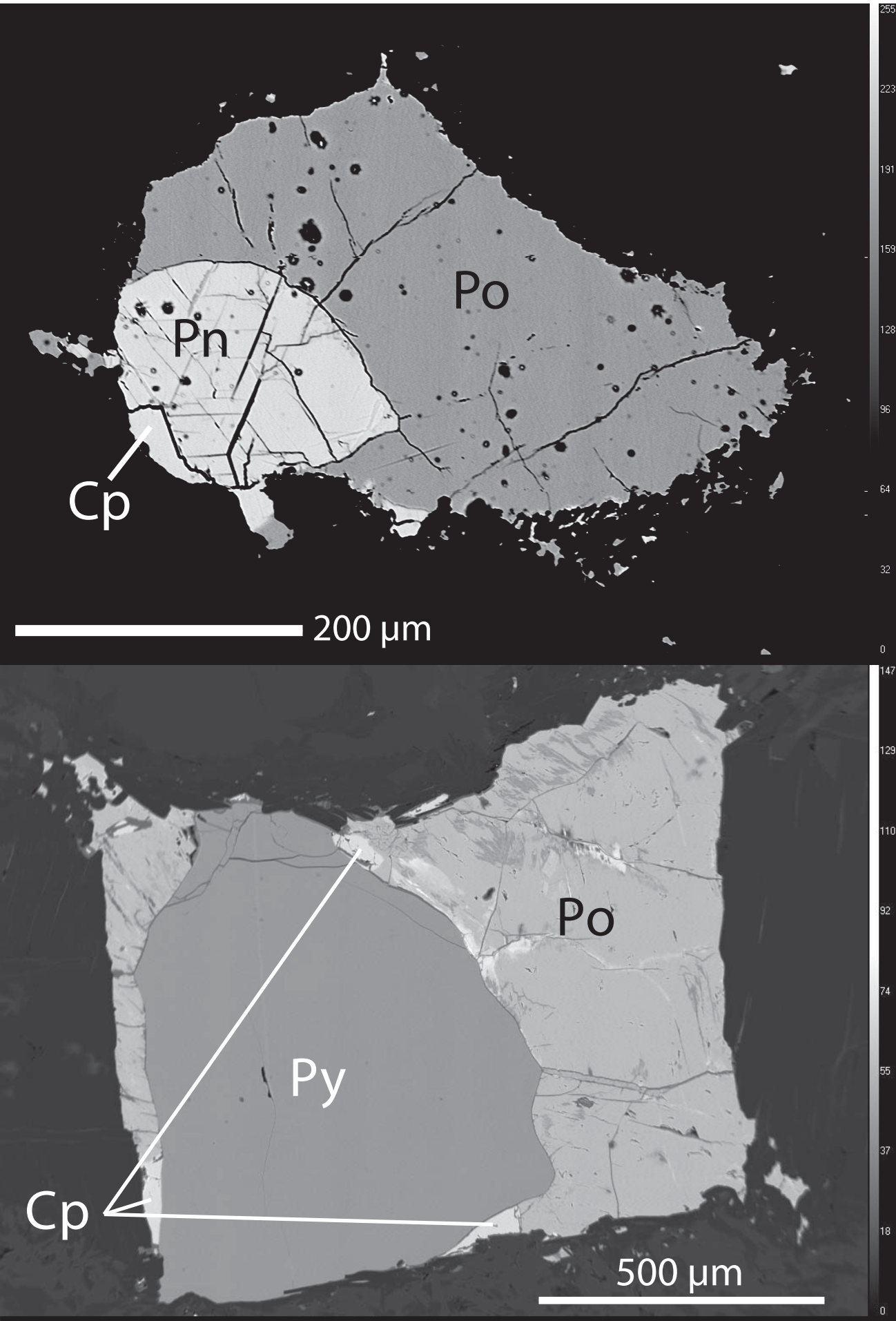

Figure 2

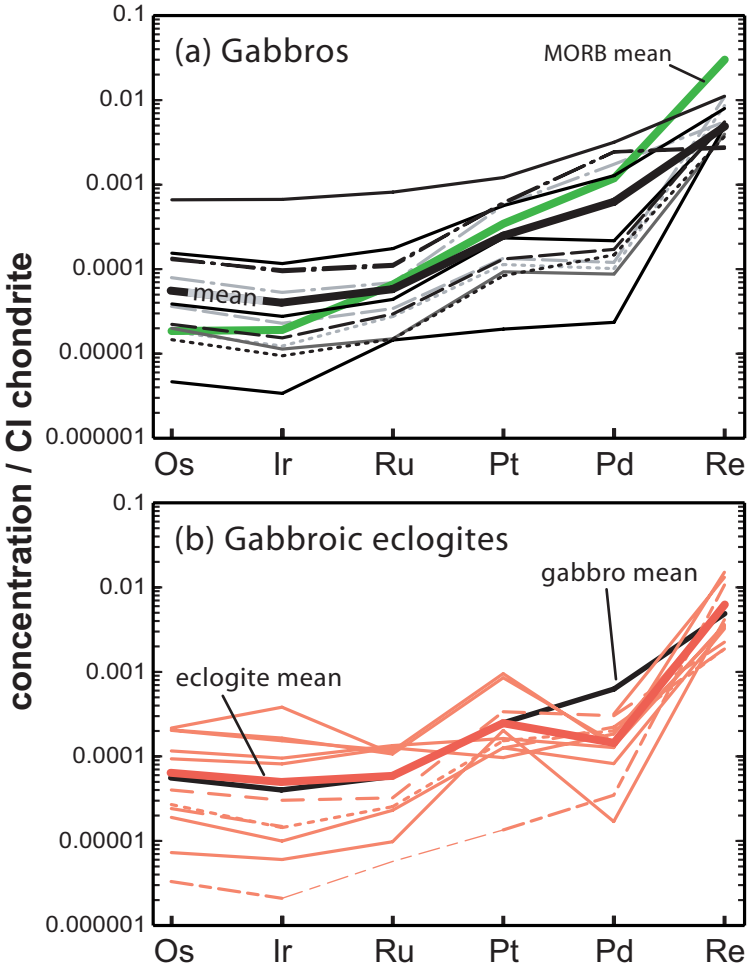

Figure 3

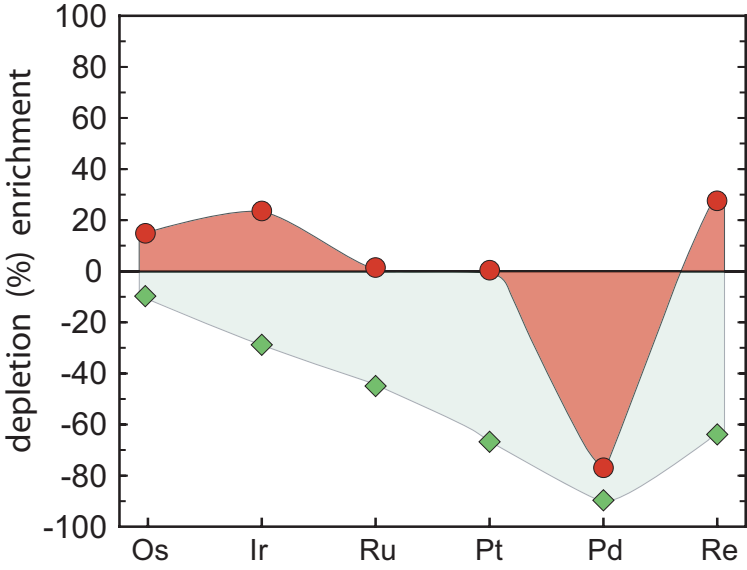

Figure 4

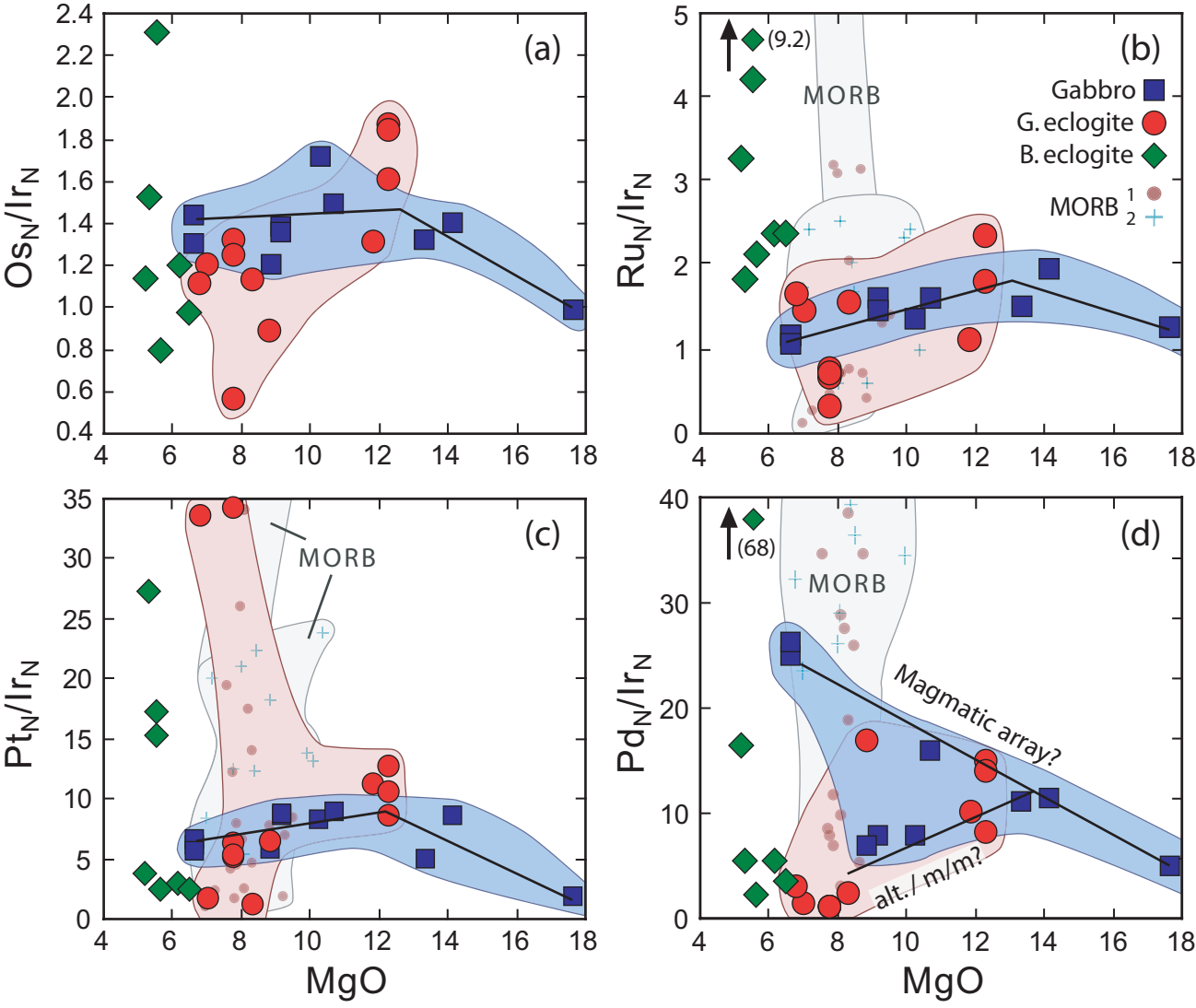

Figure 5

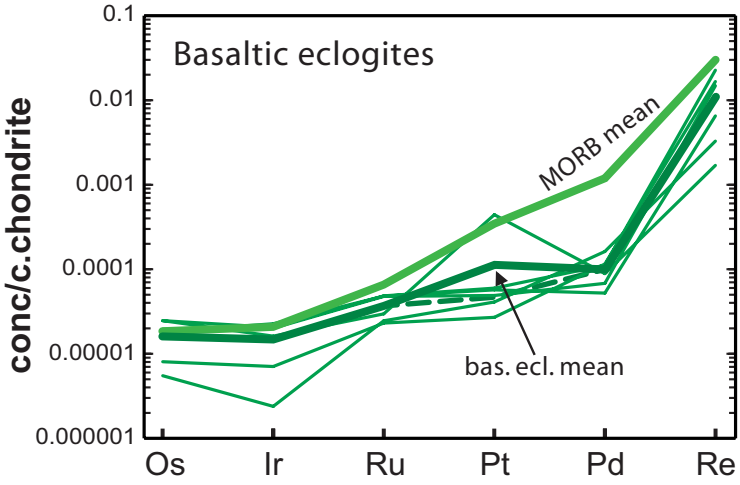

Figure 6

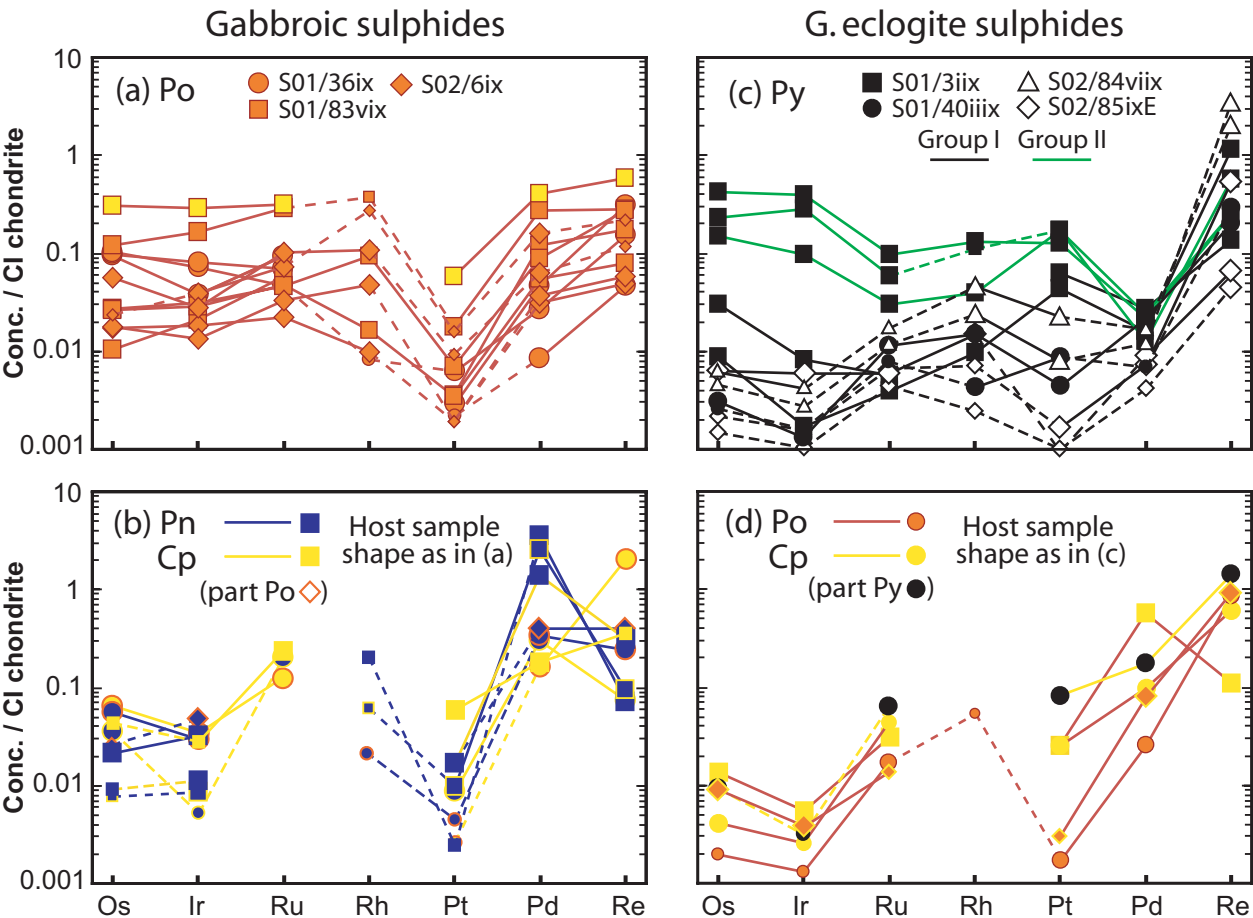
Gabbroic sulphides
G. eclogite sulphides
(a) Po
S01/36ix
S02/6ix
S01/83vix
(c) Py
S01/3iix
S01/40iiix
S02/84viix
S02/85ixE
Group I
Group II
(b) Pn
Cp
(part Po)
Host sample shape as in (a)
(d) Po
Cp
(part Py)
Host sample shape as in (c)
Conc. / CI chondrite
10
1
0.1
0.01
0.001
Os
Ir
Ru
Rh
Pt
Pd
Re

Figure 7

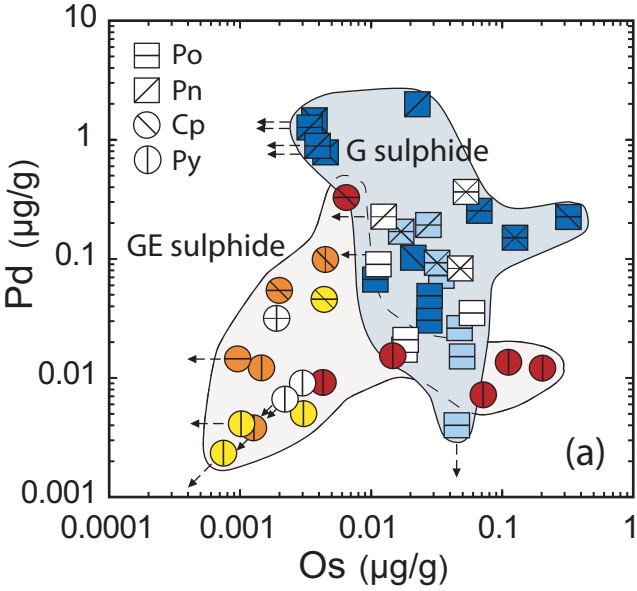
Po
Pn
Cp
Py
G sulphide
GE sulphide
(a)
Pd (µg/g)
Os (µg/g)
10
1
0.1
0.01
0.001
0.0001
0.001
0.01
0.1
1

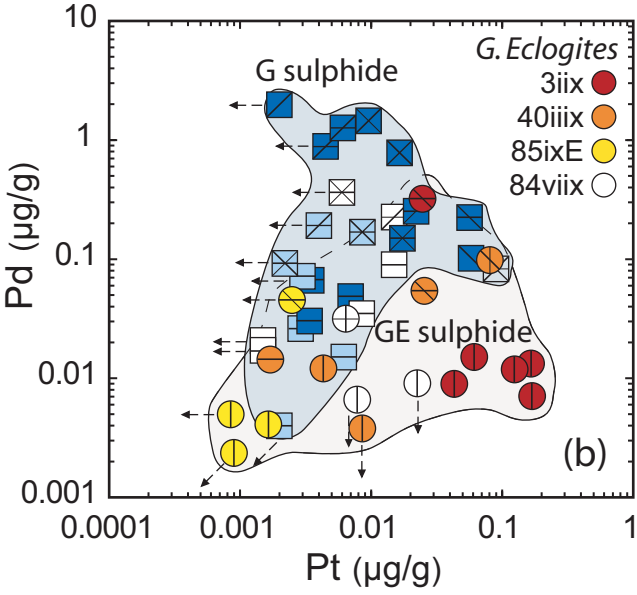
G. Eclogites
3iix
40iiix
85ixE
84viix
G sulphide
GE sulphide
(b)
Pd (µg/g)
Pt (µg/g)
10
1
0.1
0.01
0.001
0.0001
0.001
0.01
0.1
1

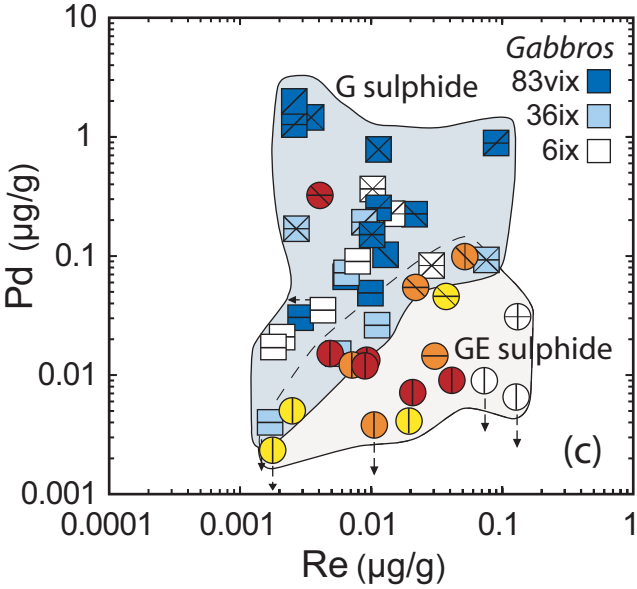
Gabbros
83vix
36ix
6ix
G sulphide
GE sulphide
(c)
Pd (µg/g)
Re (µg/g)
10
1
0.1
0.01
0.001
0.0001
0.001
0.01
0.1
1

Figure 8

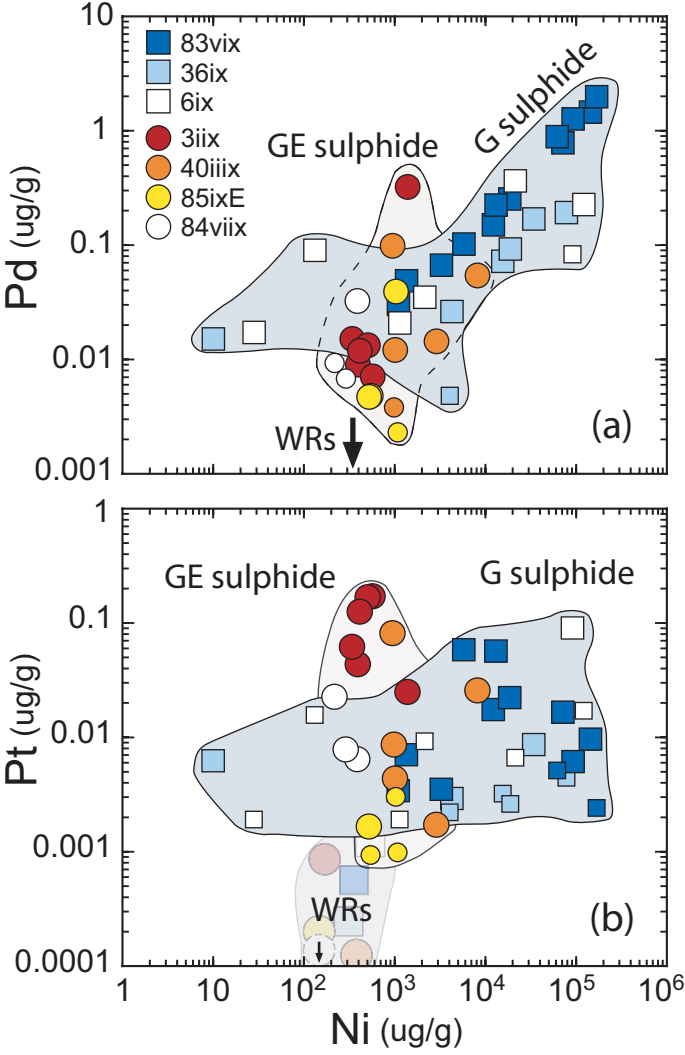
83vix
36ix
6ix
3iix
40iiix
85ixE
84viix
GE sulphide
G sulphide
WRs
(a)
Pd (ug/g)
10
1
0.1
0.01
0.001
GE sulphide
G sulphide
WRs
(b)
Pt (ug/g)
1
0.1
0.01
0.001
0.0001
1
10
10^2
10^3
10^4
10^5
10^6
Ni (ug/g)

Figure 9

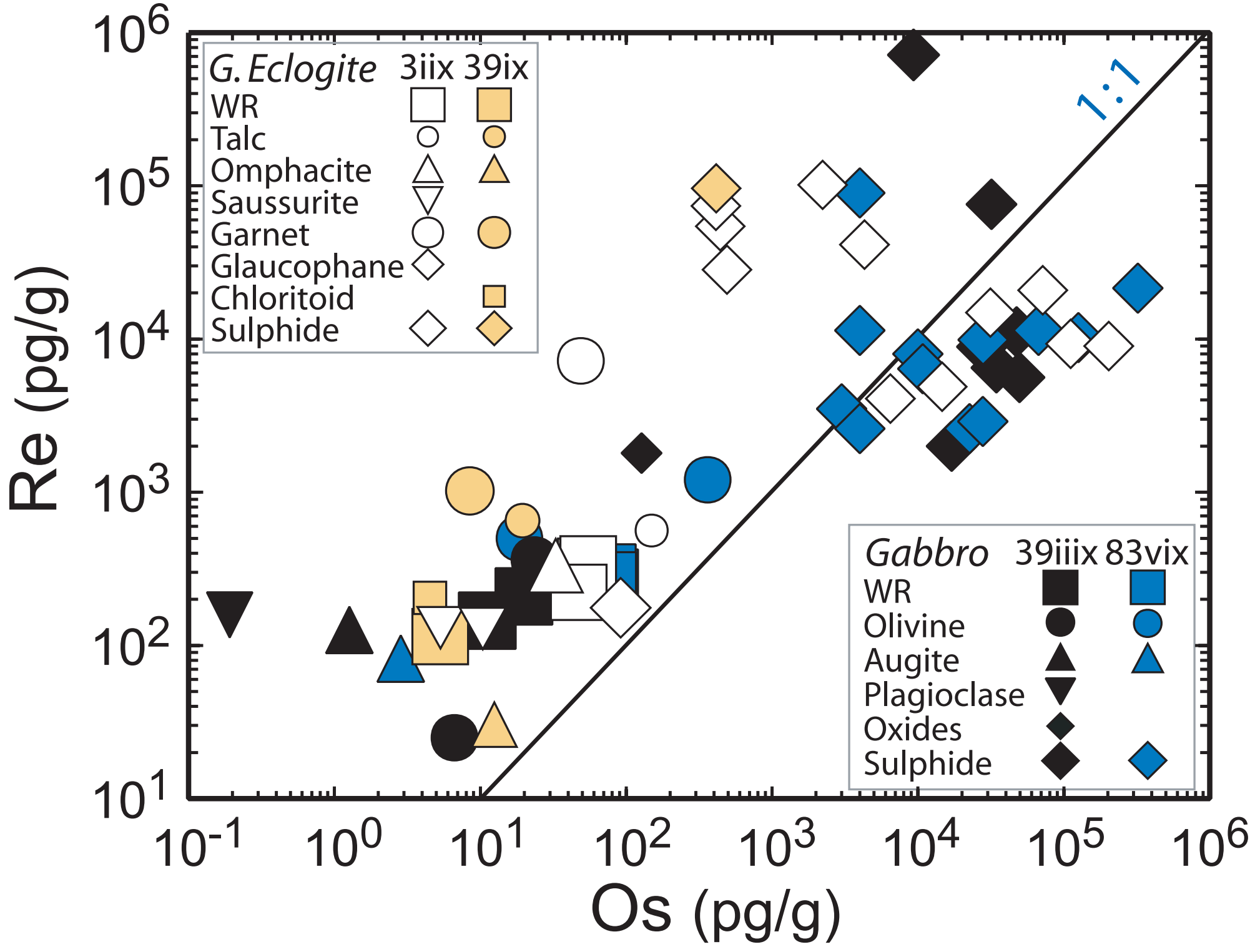
G. Eclogite
3iix
39ix
WR
Talc
Omphacite
Saussurite
Garnet
Glaucophane
Chloritoid
Sulphide
1:1
Gabbro
39iiix
83vix
WR
Olivine
Augite
Plagioclase
Oxides
Sulphide
Re (pg/g)
Os (pg/g)
10^{-1}
10^{0}
10^{1}
10^{2}
10^{3}
10^{4}
10^{5}
10^{6}

Figure 10

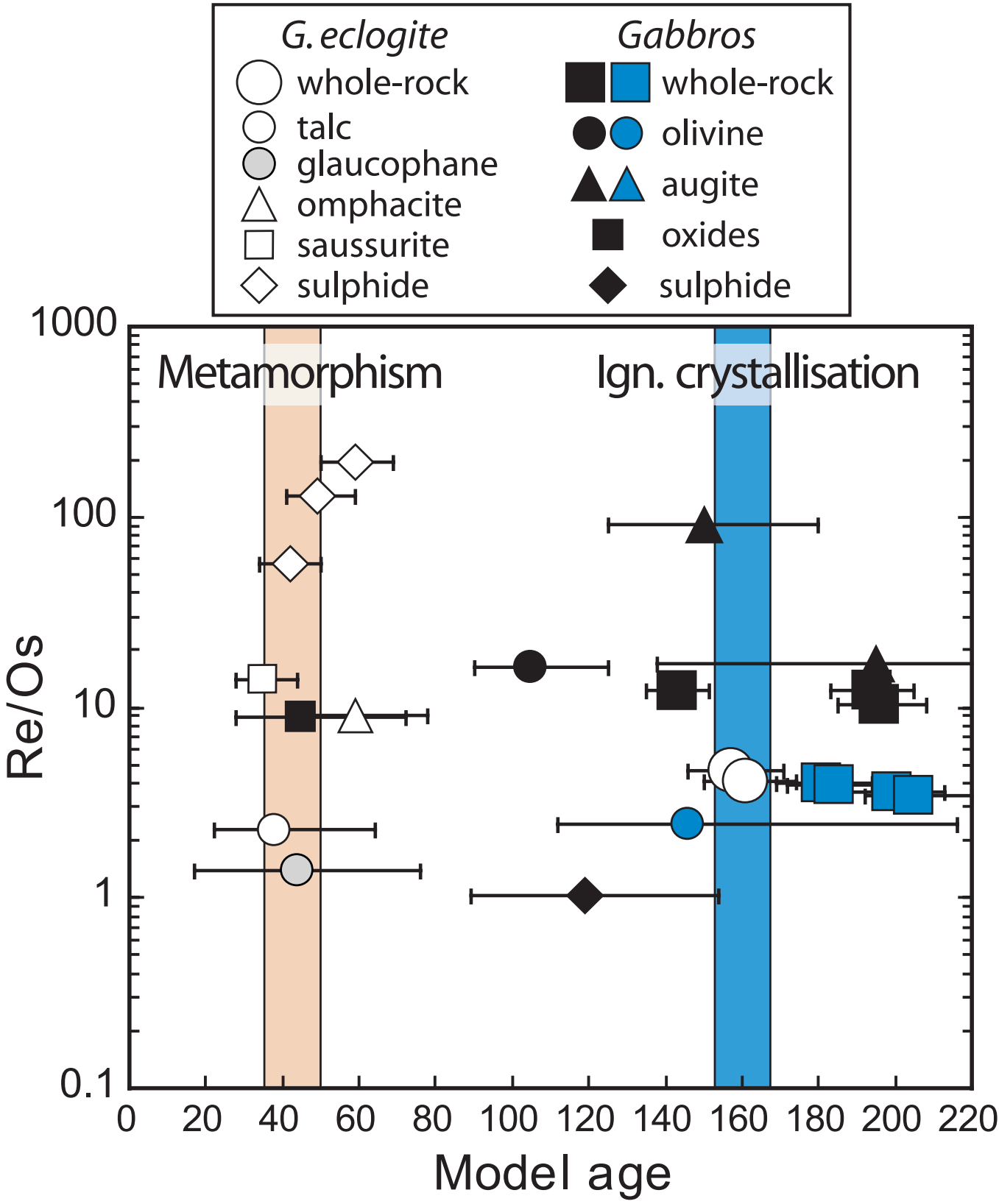
G. eclogite
whole-rock
talc
glaucophane
omphacite
saussurite
sulphide
Gabbros
whole-rock
olivine
augite
oxides
sulphide
Metamorphism
Ign. crystallisation
Re/Os
1000
100
10
1
0.1
0
20
40
60
80
100
120
140
160
180
200
220
Model age

Figure 11

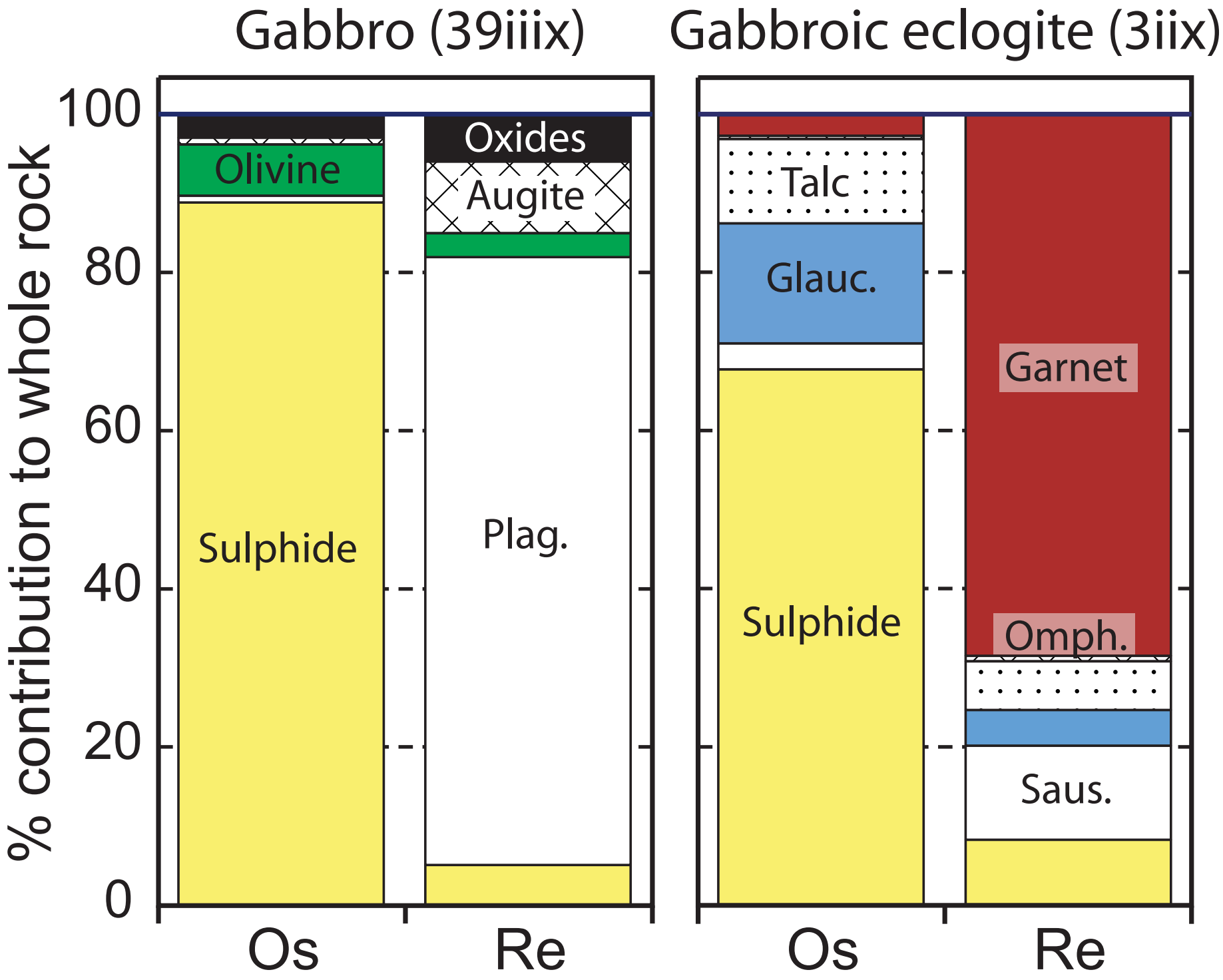
Gabbro (39iiix)
Gabbroic eclogite (3iix)
% contribution to whole rock
100
80
60
40
20
0
Olivine
Sulphide
Oxides
Augite
Plag.
Talc
Glauc.
Sulphide
Garnet
Omph.
Saus.
Os
Re
Os
Re

Figure 12

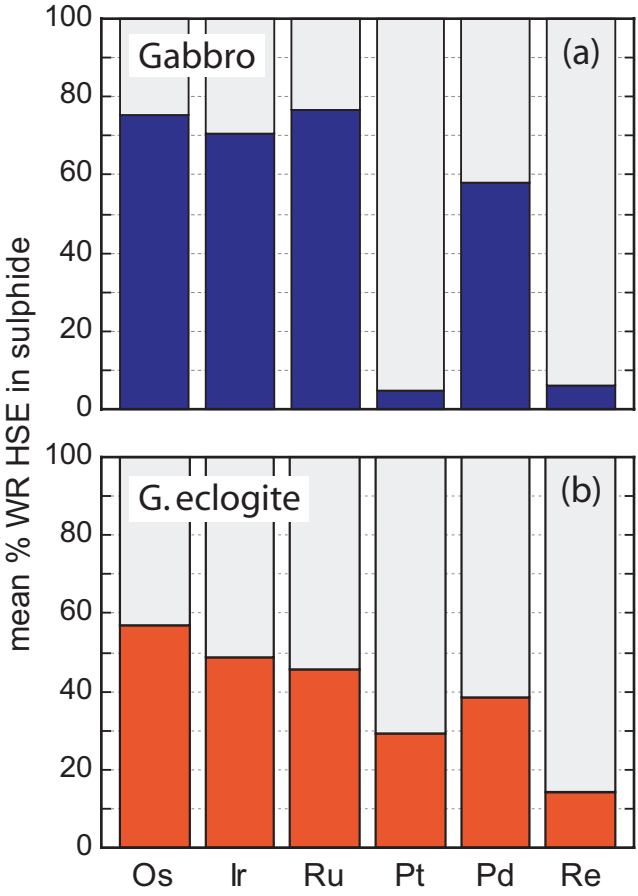

Figure 13